Cape Peninsula University of Technology
Digital Knowledge

CPUT Theses & Dissertations | Theses & Dissertations

10-1-2008

Deformation and damage analysis of composite beams equipped with polyvinylidene fluoride film sensors

Jose Emidio do Nascimento Oliveira
Cape Peninsula University of Technology

Recommended Citation

do Nascimento Oliveira, Jose Emidio, "Deformation and damage analysis of composite beams equipped with polyvinylidene fluoride film sensors" (2008). *CPUT Theses & Dissertations.* Paper 2.
http://dk.cput.ac.za/td_cput/2

This Text is brought to you for free and open access by the Theses & Dissertations at Digital Knowledge. It has been accepted for inclusion in CPUT Theses & Dissertations by an authorized administrator of Digital Knowledge. For more information, please contact barendsc@cput.ac.za.

DEFORMATION AND DAMAGE ANALYSIS OF COMPOSITE BEAMS EQUIPPED WITH POLYVINYLIDENE FLUORIDE FILM SENSORS

by

JOSE EMIDIO DO NASCIMENTO OLIVEIRA

Thesis submitted in fulfilment of the requirements for the

Masters of Technology Degree: Mechanical Engineering

in the Faculty of Engineering
at the

CAPE PENINSULA UNIVERSITY OF TECHNOLOGY

Supervisor: Prof. Dr. Bohua Sun
External-supervisor: Prof. Dr. Jasson Gryzagoridis

Cape Town
October 2008

DECLARATION

I**, José Emidio do Nascimento Oliveira,** declare that the contents of this thesis represent my own unaided work, and that the thesis has not previously been submitted for academic examination towards any qualification. Furthermore, it represents my own opinions and not necessarily those of the Cape Peninsula University of Technology.

Signed **Date**

ABSTRACT

In many engineering applications, it is desirable to know the behaviour of structures and systems under loading conditions. One reason is to help optimize the design and prevent damage and failure which might occur during in service and operation. Damage represents a serious problem which can cause catastrophic failure of structures, machines and systems. Therefore for safe operation, efficient and reliable methods for inspection and monitoring of damage are required. Different methods for health monitoring of structures such as non destructive testing (NDT) and strain gauges are widely used. These methods have proven to be efficient in terms of resolution and response. However, some disadvantages associated with them include the vicinity of the area under inspection which must be well known, equipment to acquire the necessary information is expensive and in many cases high skills are required for operation. On the other hand, advances in materials science and MEMS systems has promoted the use of new materials with piezoelectric properties. This include mainly polymeric and ceramic materials which after processed can be used for structural health monitoring. These materials offer a number of advantages such as lightweight, sensitivity, toughness, durability, and low cost.

The present research work investigates the feasibility of using a polymeric material, Polyvinylidene Fluoride (PVDF) as a sensor for deformation and defect detection in structures. The sensors are embedded in composite cantilevered type beams to detect defects at distinct locations along the beam's length. The defect detection method proposed is based on experimental tests and Finite Element simulations.

Experimental tests on defect free and beams with manufactured internal flaws were conducted. Numerical (FEM) simulations of defect free and flawed beam models containing sections of reduced elastic modulus to represent the damage were conducted using ANSYS software. The experimental tests have been used for the validation of the numerical solution. Results have shown that the defect location changes the stiffness and indeed the frequency of vibration. For flaws near the fixed end of the beams, lower frequencies are obtained as compared to flaws away from the fixed end. PVDF sensors were used to acquire the natural frequencies of the beams for the first mode of vibration. Good agreement was verified between experimental and numerical simulation results. The work has demonstrated that PVDF film sensors can be used as possible candidates for defect detection.

The analysis of the behaviour embedded PVDF sensors near the fixed end of cantilever beams, represents an initial and important step towards the application of measuring static and dynamic behaviour of structures as part of a health monitoring process.

ACKNOWLEDGEMENTS

This research work would not have been possible without the blessing and protection of God our lord, to whom I'm thankful and place on top of all.

I would like to express my sincere thanks to my supervisor Professor Bohua Sun who gave me the opportunity to join his research team and for providing all the support during this period. The introduction to the field of Smart Materials and Structures and assistance during the problem formulation and valid suggestions and opinions provided by professor Sun are highly appreciated.

I am truly grateful to my external supervisor Professor Jasson Gryzagoridis from the University of Cape Town, who guided me unconditionally throughout this work. His patience, encouragement and support in all stages of the project were of very great value and are highly acknowledged.

I wish to thanks the Advanced Manufacturing Technology Strategies (AMTS) of South Africa for the involvement and financial support to this project.

The staff of the Mechanical Engineering department is also acknowledged specially, Professor G.Oliver (Masters Degree programme coordinator for mechanical engineering) for his help with Finite Element Analysis and course work and Dr. O. Philander (Head of the Smart Alignment Group of the Centre for Applied Research and Technology) for the valid discussions and support during the problem formulation.

I also wish to thank Mr. W. Kohffler for his wiliness to help with experimental equipment and set-up.

A big recognition and appreciation is extended to my family and friends for their love, their belief and their support both morally and materially during this phase of my life.

DEDICATION

To My Parents: Jose and Luzia
My Brother, Sisters and Girlfriend: Amilcar, Mariete, Florinda, Neide and Maria

For their love, encouragement, support and our union during the happy and difficulty moments

TABLE OF CONTENTS

DECLARATION II
ABSTRACT III
ACKNOWLEDGMENTS IV
DEDICATION V
LIST OF FIGURES IX
LIST OF TABLES XII
LIST OF APPENDICES XIII
GLOSSARY XIV
NOMENCLATURE XV

CHAPTER ONE: INTRODUCTION

1.1 Motivation 1
1.2 Problem Statement 2
1.3 Research Objectives 4
1.4 Research Approach and Methodology 4
1.5 Dissertation Outline 5
1.6 Smart Materials and Structures 6
1.6.1 Classification of Smart Materials 6
1.6.2 Application Fields of Smart Materials and Structures 8
1.7 Overview of Structural Health Monitoring 9
1.7.1 Main Requirements of Structural Health System 9
1.7.2 Methods used for Structural Health Monitoring 10
1.7.3 Objectives of Structural Health Monitoring Process 13

CHAPTER TWO: LITERATURE REVIEW

2.1 Introduction 16
2.1.1 History of Piezoelectricity 16
2.2 Piezoelectric Materials and Systems 17
2.3 Source of Piezoelectric Effect: Polarisation 18
2.4 Piezoelectric Constitutive Equations 20
2.5 Properties of Piezoelectric Material 22
2.5.1 Directions and Constants 22

2.5.2 Pyroelectricity and Ferroelectricity 25
2.6 Production Process of PVDF Films 26
2.6.1 Material Properties 27
2.7 Sensor Fabrication Method 28
2.7.1 Coat Etching Method 28
2.7.2 Conductive Epoxy Method 29
2.7.3 Copper Foil Tape Method 30
2.8 Sensor Embedding Techniques and Material Integrity 30
2.9 Sensor Response Measurements 32

CHAPTER THREE: BENDING DEFORMATION OF BEAMS EQUIPPED WITH SENSORS

3.1 Introduction 34
3.2 Deformation of Smart Composite Beam 34
3.2.1 Derivation of Internal and External Bending Moment 35
3.2.2 Strain-Stress State of Smart Composite Beam 42
3.2.3 Bending Stiffness of Composite Beam 44
3.3 Bending Curvature to Voltage Relationship 44
3.3.1 Static Sensor Equations 44
3.3.2 Dynamic Sensor Equations 46

CHAPTER FOUR: DAMAGE ANALYSIS

4.1 Introduction 48
4.2 Interpretation of Damage 48
4.3 Types of Damage and its Origin 49
4.3.1 Material Imperfection 49
4.3.2 Manufacturing Process 50
4.3.3 Operation 50
4.3.4 Environmental Conditions 50
4.4 Effects of Structural Damage 51
4.5 Formulation of Elastic Material Damage 52
4.6 Damage Detection Model Approach 53
4.7 Damage Analysis in Cantilever Beams 54
4.7.1 Static Equations 54
4.7.2 Vibration Equations 55

CHAPTER FIVE: EXPERIMENTAL AND NUMERICAL INVESTIGATION

5.1 Introduction 58
5.2 Fabrication of Defect Free and Flawed beams with Embedded Sensors 58
5.2.1 Making the Sensors from PVDF Films 58
5.2.2 Material Preparation and Fabrication Method 59
5.3 Experimental Procedure 61
5.3.1 Measurement of Static Displacement 61
5.3.2 Measurement of Frequency Response 62
5.3.3 Results and Discussion for Static Displacement Measurements 64
5.3.4 Results and Discussion for Frequency Response Measurements 64
5.4 Numerical FE Simulation for Predicting the Beam's Behaviour 66
5.4.1 Software Description 66
5.4.2 Finite Element Model and Analysis Procedure 66
5.4.3 Static and Dynamic FE Equations 71
5.5 Case Study: Effect of Flaw Size and Position on the Response of Cantilever Beam 71
5.5.1 Simulation Results under Static Loading 72
5.5.2 Simulation Results under Dynamic Loading 74
5.6 Comparison Between Experimental Results and FE 78

CHAPTER SIX: CONCLUSIONS AND RECOMMENDATIONS FOR FUTURE WORK

6.1 Introduction 79
6.2 Research Outcomes 79
6.3 Recommendations for Future Work 80

REFERENCES 81

BIBLIOGRAPHY 85

APPENDICES 87

LIST OF FIGURES

CHAPTER 1

Figure 1.1: Smart material and structure network 8

Figure 1.2: Typical Health Monitoring Procedure 10

Figure 1.3: Structural Heath Monitoring objectives diagram 13

CHAPTER 2

Figure 2.1: Pierre and Jacques Curie 1880 16

Figure 2.2: Polarised and unpolarised forms of PZT 19

Figure 2.3: Chemical structure and polarisation phase of PVDF 19

Figure 2.4: Conventional Directions for Piezoelectric materials 22

Figure 2.5: Applied Force Resulting in Voltage Generation 24

Figure 2.6: Typical Hysteresis Loop for PVDF 26

Figure 2.7: characteristics of Typical PVDF film 27

Figure 2.8: Etching of Conductive Coating to Create an Effective Sensor 29

Figure 2.9: PVDF Film Sensor with Crimp Connector 29

Figure 2.10: Copper Tape Attachment 30

CHAPTER 3

Figure 3.1: Beam with Embedded Piezoelectric Film 35

Figure 3.2: A Differential Segment of a Beam in Pure Bending 36

Figure 3.3: Cantilever Beam with Transversely Applied Load and Geometric System 38

Figure 3.4: Free Body and Bending Moment Diagram of a Beam 41

Figure 3.5: Stress and Strain Distribution in the Beam due to External Loading 43

Figure 3.6: Rectangular Sensor Strip 45

CHAPTER 4

Figure 4.1: Interface crack delamination of composite beam 51

CHAPTER 5

Figure 5.1: Sensor from PVDF Film 59

Figure 5.2: Specimens Material 60

Figure 5.3: Components used for specimens Fabrication 60

Figure 5.4: Fabricated Defect Free and Flawed Beams 61

Figure 5.5: Experimental Set-up for Displacement Measurements 62

Figure 5.6: Experimental Set-up for Dynamic Measurements 63

Figure 5.7: Apparent Elastic Modulus for Defect free and Flawed Beams 64

Figure 5.8: Frequency of Flawed Beams as a Function of Position 65

Figure 5.9: Damage Model of the Beam 67

Figure 5.10: Defect Free and Flawed Beam Models in ANSYS 68

Figure 5.11: Flawed Beam Model and Contact Parameter 69

Figure 5.12: Mesh of Defect Free and Flawed Beams 70

Figure 5.13: Load Vs Free end Displacement for Flawed beams at X_i = 0 and 23.75 mm 72

Figure 5.14: Load Vs Free end Displacement for Flawed beams at X_i = 0 and 47.5 mm 72

Figure 5.15: Load Vs Free end Displacement for Flawed beams at X_i = 0 and 82.5 mm 73

Figure 5.16: Load Vs Free end Displacement for Flawed beams at X_i = 0 and 117.5 mm 73

Figure 5.17: Defect Free and Flawed Beams at X_i = 23.75mm 74

Figure 5.18: Flawed Beams at X_i = 47.5mm and 82.5mm under Dynamic Loading 75

Figure 5.19: Flawed Beam at X_i = 117.5mm under Dynamic Loading 76

Figure 5.20: First Mode Frequency Vs Flaw Position 76

Figure 5.21: Frequency Vs Flaw Position: Experimental and FE Results 78

LIST OF TABLES

Table 1.1: Summary of Structural Health Monitoring System Capabilities 14

Table 2.1: Typical Properties of Piezoelectric Materials 25

Table 5.1: Sensor Properties 59

Table 5.2: Material Properties of Composite Beam 69

Table 5.3: FE and Experimental Results for Defect Free and Flawed Beams 78

APPENDICES

Appendix A: Experimental Measurements under Static Loading 87

Appendix B: Experimental Measurements under Dynamic Loading 89

Appendix C: FE Results for Beams under Static Loading 90

Appendix D: FE Results for Beams under Dynamic Loading 91

GLOSSARY

ACRONYMS	MEANING
CFD	Computational Fluid Dynamics
ER	Electro Rheological
FEM	Finite Element Method
GSM	Gapped Smoothing Method
GFD	Generalised Fractal Dimension
IRT	Infrared Thermography
LEFM	Linear Elastic Fracture Mechanics
MEMS	Micro-Electro Mechanical Systems
MR	Magneto Rheological
NDT	Non – Destructive Testing
PMMA	Poly Methyl Methacrylate
PVDF	Polyvinylidene Fluoride
PZT	Lead Zirconate Titanate
PFRC	Fibre Reinforced Composite
SEM	Strain Energy Method
SHM	Structural Health Monitoring

NOMENCLATURE

GREEK LETTERS & SYMBOLS

β – Percentage of stiffness loss parameter [dimensionless]

ε_b – Strain in the beam [dimensionless]

ε_s – Strain in the sensor [dimensionless]

σ – Stress in the beam [MPa]

ρ – Density of beam material [kg/m^3]

v – Poisson's ratio [dimensionless]

λ_i – eigen value for different modes of vibration [dimensionless]

ω – Circular frequency [rad/s]

e_{31} – Dielectric coefficient of PVDF sensor material [C/m^2]

a_2 - a_1 – Difference between the furthest and closest distance to flaw area [m]

B – Width of the beam [m]

E_U – Elastic modulus of the beam in the undamaged state [GPa]

E_D – Elastic modulus of the beam in the damaged state {GPa]

f_U – Frequency of the beam in the undamaged state [Hz]

f_D – Frequency of the beam in the damaged state [Hz]

H – Height of the beam [m]

k_U – Stiffness of beam in undamaged state [k/m]

k_D – Stiffness of the beam in the damaged state [k/m]

L_b – Length of the beam [m]

L_D – Length of flaw area [m]

L_s – Length of the sensor [m]

M_0– Internal moment at neutral axis [Nm]

M_E – External moment due to applied loading [Nm]

P – Applied Load [N]

X_i – Flaw position from fixed end of the beam to centre of flaw area [m]

CHAPTER ONE

INTRODUCTION

1.1 Motivation

The current advances in materials science and Micro Electro-Mechanical Systems (MEMS), is promoting the use of certain new classes of materials. Examples are piezoelectric and piezoceramic materials such as Polyvinylidene Fluoride (PVDF), Lead Zirconate Titanate (PZT) and Quartz which have unusual properties not found in many other materials. These mainly include sensing and actuating (self-power) capabilities which can be used to monitor the static and dynamic behaviour of structures and systems.

In order to ensure good operation of structures and systems and to avoid failure and damage, information about the structure's behaviour under loading conditions needs to be monitored in real time. The conventional non-destructive testing (NDT) methods for inspection of structures such as x-rays, C-scanning, ultrasound, infrared imaging and radiography offer good performance in terms of resolution and response. However, some of the disadvantages associated with these technologies is that the vicinity of the area to be inspected needs to be well known, the equipment for acquiring the necessary information is expensive (need physical connection or power supply), it is time consuming and skills is required to operate them. These factors make the technologies not entirely appropriate for monitoring structures such as aircraft (i.e. wings, flappers) and helicopters (i.e. rotor blades) which require regular inspection due to their operating conditions. An alternative for this situation consists of the integration of inexpensive and reliable adaptive materials in to structures and systems thus enabling real time (in-operation) response to changing conditions. Piezoelectric materials (which are used as adaptive) such as PVDF offer the advantage of requiring no power to operate, provide quick response and can be incorporated directly in to the structure to detect deformation and damage. In this way, information about structural behaviour can be obtained and monitored reducing the resources needed for inspection and repair (Chen & Wang, 2004).Technologies using adaptive materials for inspection and monitoring of structures are been used worldwide (mainly in developed countries) in different industrial sectors but not yet in South Africa. Therefore, it is important to investigate their capabilities and means of integration in to structures and systems to be applicable to the South Africa industry.

1.2 Problem Statement

Deformation and damage can become serious to the point of causing failure of metallic and composite structures. Normally, they reduce the strength (flexural rigidity) and the load carrying capacity which makes the structure weaker. Therefore, for safe operation it is necessary to use methods for identification and monitoring of damage. Polyvinylidene Fluoride (PVDF) films have been used as sensing and actuating devices. Their characteristics such as light weight, sensitivity, toughness, durability and flexibility to be made into different shapes, makes them good candidates for structural health monitoring (Bar-Cohen & Lih, 1996). In order to use PVDF film as a sensor it needs to be incorporated in a structure so that it can react to the behaviour of the structure. One way to interpret structural behaviour and hence defects, damage or failure is to measure the voltage output of the sensor due to the structures displacement as a result of an applied external stimulus such as force, temperature, humidity etc.

Structural health monitoring has been an active researched area over the past years. Keilers & Chang (1995) proposed a model for the control of beams using distributed sensors and actuators mounted on the top and bottom surfaces. The model was used to perform a parametric identification of damage occurring at the neutral axis of built in and simply supported beams. Luo & Hanagud (1999), carried research on the applicability of PVDF film sensors for damage detection in aluminium alloy beams. The investigation aimed to experimentally examine the structural dynamic response using removable sensors in both damaged and undamaged beams.

A one dimensional model to detect a single defect (delamination) in a laminated composite beam using piezoelectric fiber reinforced composite (PFRC) sensor/actuator layer was proposed by Tan & Tong (2003). The model was used to predict the first three mode frequencies, and the sensor response along the beam when excited by the PFRC actuator. Ling & Cheng (2005) proposed a model to identify damage by computing the eigenvalues for a damaged composite beam without considering sensors and actuators. The approach however was limited to the estimation of the amplitude of the vibrating frequency modes of the beams.

Gama and Morikawa (2007) reported the results of an experimental study on the application of piezoelectric dynamic strain sensors for crack length measurement in fracture mechanics specimens. The performance of the piezoelectric sensors was assessed through fatigue crack propagation tests in compact tension (CT) specimens. Sensors of polarized polyvinilidene fluoride polymer (PVDF) were

bonded to the back face of CT specimens, in the same manner as the electrical resistance strain gages installed for crack length measurement. The results showed that, mainly due to its high sensitivity to strain, the use of piezoelectric materials as dynamic strain sensors can contribute to the experimental investigation in the field of fracture mechanics.

An important aspect to consider is the incorporation of the piezoelectric material in to the monitoring structure which dictates its effectiveness as sensing and actuating devices. Piezoelectric sensors/actuators can be incorporated in to a structure either by embedding (sandwiching) them or mounting on to the surface of the host structure. If piezoelectric materials are mounted properly to a structure (using adequate type of adhesive), structural deformations can be induced by applying a voltage to the materials, employing them as actuators. On the other hand, they can be employed as sensors since deformations of a structure would cause the deformed piezoelectric material to produce an electric charge. The extent of structural deformation can be observed by measuring the electrical voltage the materials produce. However, surface mounted sensors are likely to get damaged or peel due to high longitudinal stresses which might developed at the interface (in the case of brittle piezoelectric materials such as PZT) or by contact with surrounding objects (in the case of flexible piezoelectric materials such as PVDF). The embedding method seems to alleviate this problem.

In this research, embedded PVDF sensors are used to investigate deformation and defects in cantilever beams. The Euler Bernoulli beam theory is considered. Static and dynamic analyses are performed to emphasise the relationship between beam deformation and sensor response. Furthermore, the defect detention capability of the sensor is demonstrated through experimentation with composite beams.

1.3 Research Objectives

The aim of this research is to investigate the viability of using embedded PVDF sensors to monitor the response of defect free and beams with internal flaws. To achieve this, the following tasks were undertaken:

I. Mathematical formulation describing the beam interaction with sensor and its response

II. Numerical model analysis and simulation of defect free and beams with flaws

III. Manufacturing of defect free and flawed specimens

IV. Experimental investigation for validation of the numerical model

1.4 Research Approach and Methodology

A description of the research method used in this work follows: A literature survey which was initially conducted on the different types of beam deformation such as bending, twisting and buckling as well as defects found due to material imperfections, fabrication methods and operation which initiate and grow during the life time of the structure. Various techniques used in monitoring structural health were identified. The survey was extended to piezoelectric materials, their characteristics and usage as sensors and actuators as well as their integration into structures. The survey also included various techniques that measure the sensor's response to applied loading.

Due to the nature of this research, the approach consists of experimental and numerical methods. The experimental method consists of the design and manufacturing of beam models embedded with PVDF sensors and containing internal localized defects. With the assistance of laboratory equipment, static and dynamic measurements were carried out to detect the presence of defects through sensing of the beams behaviour which is interpreted by the embedded PVDF sensors. The numerical method encompasses the formulation of a model for the cantilever beam containing defects. The model can accommodate different simulated flaw locations, to obtain its behaviour under load conditions. In order to verify the numerical method, the experimental results were used.

1.5 Dissertation Outline

This thesis is presented in six chapters. The present one is an introductory chapter with statement of the motivation for this work, problem description, research methodology and an overview of smart materials and structures as well as Structural Health Monitoring. One of the aims of this chapter is to introduce the reader to the capabilities of MEMS and smart materials and systems as potential candidates for control and monitoring of structures.

In chapter 2, the theory of piezoelectric materials with emphasis on their properties, characterisation and application fields is presented. This chapter is aimed to provide a good background on piezoelectric materials with focus on PVDF.

Chapter 3 presents the bending deformation of beams with incorporated sensors. Assumptions based on the classical beam theory are used to describe the interaction between the beam and the piezoelectric sensor. Stress, strain and displacement are emphasised and the relationship between beam curvature and sensor response is established.

Chapter 4 is focused on damage analysis. An Interpretation of damage types and origin is discussed. Models containing defects are briefly described and analysis of defect free and flawed beams is presented.

Experimental investigation of cantilever beams with embedded sensors for defect detection is presented in chapter 5. The results obtained are used to validate a FE model which was constructed and simulated to predict the effects of flaws in the cantilever beam's behaviour.

Concluding remarks and recommendations for future work are discussed in chapter 6.

1.6 Smart Materials and Structures

The use of advanced structures with integrated control and monitoring capabilities is becoming more common due to the rapid development of “smart materials”. Smart materials are described as a group of materials with the ability to perform specific functions such as sensing and actuating. This ability is due to their physical and chemical composition which enables them to behave as self controlling materials. In other words, these materials which are also called intelligent, active or adaptive are materials that respond upon application of externally applied forces (Sun, 2003).

According to Srinivasan (2001), “an intelligent or smart structure is capable of altering its mechanical states, i.e. position or velocity or its mechanical characteristic i.e. stiffness or damping in response to applied external conditions”.

Smart structures (containing smart materials) are man-made structures with built in monitoring and control functions. These structures normally incorporate one or more of the following features:

1. Sensors which are made from smart materials embedded or else bonded on a structure to sense changes due to external stimuli.

2. Actuators which are also made from smart materials embedded or bonded on a structure. These actuators are typically excited by an external stimulus, such as electrical current in order to change the geometrical configuration, stiffness and energy properties of the structure in a controlled manner.

The reliability of these materials and their integration into structures and systems to be used as control and repair unit is one of today’s main focus in the science and technology fields.

1.6.1 Classification of Smart Materials

Smart materials can be grouped in to the following categories:

Piezoelectric materials: are solid materials which generate a charge in response to a mechanical deformation as well as exhibit the opposite effect, i.e. they deform when subjected to an applied current. Normally these materials are used as either actuators or sensors in the development of smart structures.

Magnetostrictive materials: are also solid materials which develop large mechanical deformations when subjected to an external magnetic field. The magnetostriction phenomenon is attributed to the rotations of small magnetic domains in the material, which are randomly-orientated when the material is exposed to a magnetic field. The orientation of these small domains by the imposition of the magnetic field results in the development of a strain field. As the intensity of the magnetic field is increased, more and more magnetic domains orient themselves (Srinivasan, 2001). A typical magnetostrictive material is Terfenol-D.

Shape memory alloys: are metals that deform plastically at one temperature and completely recover their original undeformed state upon raising their temperature above an alloy specific transformation temperature. A characteristic of these alloys is that the crystal structure undergoes a phase transformation which results in shape changes. Shape memory alloys are present in two forms: martensite and austenite. It deforms to martensitic form with low temperature and regains its original shape in its austenite form when heated (high temperature). i.e: Nitinol (TiNi).

Electrorheological (ER) and Magnetorheological (MR) fluids: are typically suspensions of micron sized hydrophilic particles in suitable hydrophobic carrier liquids, which undergo significant instantaneous reversible changes in their mechanical properties, such as mass distribution energy dispassion character, when subjected to an electric field for the (ER) and when subjected to magnetic field for (MR) fluids (Srinivasan, 2001).

Electrostrictive materials: are similar to magnetostrictive materials because they also develop mechanical deformation when subjected to an external electric field. The electrostrictive phenomenon is attributed to the rotation of small electrical domains in the material when an external electrical field is imposed upon them. In the absent of this field, the domains are randomly orientated. The alignment of this electric domains results in the development of a deformation field in the material. The ceramic compound, lead-magnesium-niobate (PMN), is a typical electrostrictive material.

Optical fibers: are fibers that use intensity, phase, frequency or polarization of light for measurement of temperature, strain, magnetic or electric fields, pressure and other measurable quantities. Optical fibers serve a dual role in smart structures because they not only provide a sensing capability but also a transmission medium for signals. The light signal is transmitted through the fiber from the region which is subjected to the external stimulus i.e: Bragg grating in optical fibers is typically used

as sensors for deformation.

While optical fibers are used primarily as sensors, the electrostrictive materials, shape memory alloys and electrorheological/ magnetorheological fluids are normally used as actuators. However, in certain applications some of the materials are rather used as sensors which is the case of PVDF due to its high flexibility and sensitivity. The interaction between smart materials and structure is shown below.

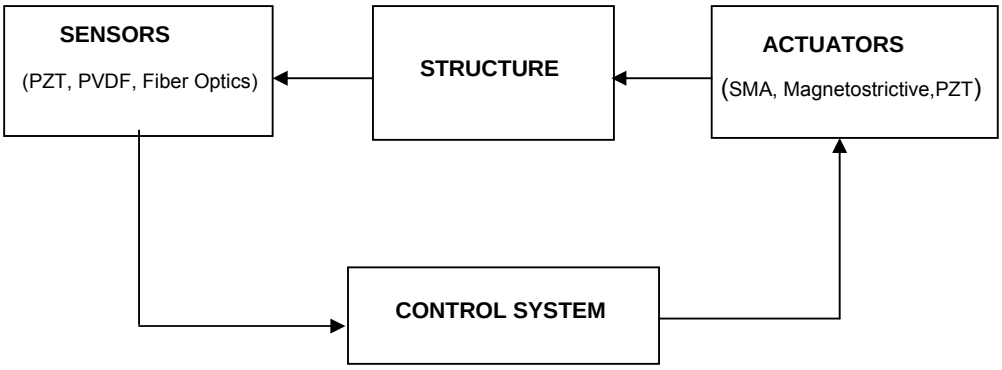

Figure 1.1: Smart material and structure network

One way to preserve its integrity so that a structure can continue to be used for its designed function is by ensuring that an effective and adequate health monitoring system exists. Piezoelectric, magnetostrictive, electrostrictive, shape memory alloys electrorheological/magnetorheological and optical fibers have demonstrated capabilities to be used as such.

1.6.2 Application Fields for Smart Materials and Structures

Smart materials can be used for many applications. The benefits of using these materials is still in its development phase, however significant achievements in many industrial sectors have been obtained. Some of the applications are summarized here (Piezo Films 2006; George, 2007):

Automotive: the automotive industry has relied on the use of sensors made of smart materials such as PZT and PVDF for impact safety actuation on cars (air bags), the monitoring of bearings and clutch wear, distance sensing etc.

Aerospace/Military: the aerospace and military industry was one of the first to explore the capabilities of smart piezoelectric materials for sensing and actuation applications. Sensors were incorporated in aircraft structures to detect and monitor damage due to aerodynamic forces. On the military side advances in military

weapons and transport systems (submarines) make vast use of these materials.

Industrial: In the industrial sector, the focus includes mainly switches such as: acoustic, singing and coin counter switches, keypad and snap action and in robotics for tactile sensors, micropositioners, safety mats and bumper impact.

Instrumentation: In the instrumentation field, the sensors made of these materials are found to be very useful in controlling parameters such as pressure, temperature and humidity levels as well as vibration and acoustic control. Examples include:

Machine monitoring: accelerometers, contact microphones and dynamic strain gauges

Oil exploration field: hydrophones and seismic geophones

Weather analysis: rain intensity, wind velocity and hail detection

Medical: The medical sector also has seen significant developments in the use of smart piezoelectric materials to monitor and operate equipment such as:

Diagnostics: blood pressure cuff, respiratory air flow, patient bed monitor, pulse counter and stethoscope

Ultrasound: field imaging, prostate, hydrophone and calibration probes

Infrastructure Design and construction: In this field, these materials have been used for buildings: earthquake resistance, smart windows that sense weather changes and bridges: monitoring of strains, deflections and vibration characteristics.

1.7 Overview of Structural Health Monitoring (SHM)

SHM is the name attributed to the process of evaluating the physical condition of a structure. It consists of methods used to collect data about structural behaviour to provide an indication when anomalies are present. This approach helps to update the condition of the structure including the detection of changes in materials properties. The present work is focused towards the use of smart sensors and techniques to detect deformation and damage in structures which is part of a SHM process.

1.7.1 Main Requirements of a SHM System

The main requirements for health monitoring of a structure based on smart materials is that it should be made or contain a sensor – to sense any change in structural behaviour, actuator- to actuate the structure giving it the required motion, data acquisition system – to gather all the necessary information from the sensors and actuators and processing unit – to analyse the acquired data in a meaningful manner

to describe the current state of the structure. Indeed a smart structure is a structure with a build in health monitoring capability. This concept can be illustrated with aid of the figure shown below.

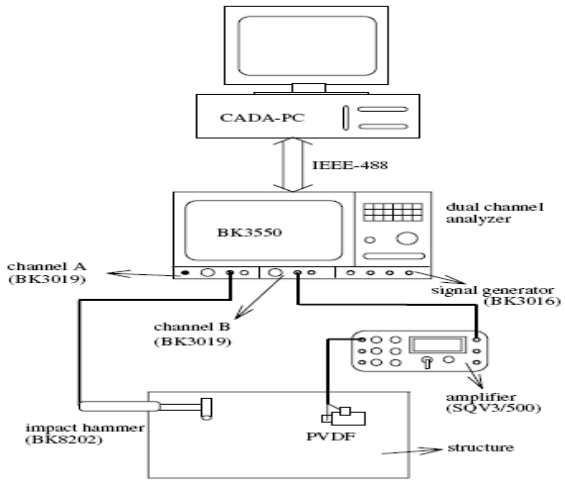

Fig 1.2: Typical Health monitoring procedure i.e. plate (Cheng & Wang, 2004)

As seen from the figure, the attached sensor is used to monitor the dynamic behaviour of the plate due to a hammer impact. In this case the hammer is used as an actuator. The impact of the hammer would cause the structure to vibrate freely. The data acquisition system includes an amplifier (to amplify the signal produced by the sensor), dual channel analyser (to store and analyse the structure response) and a PC with interface software to process and display the structure's behaviour. The above demonstration would be a typical example of monitoring the dynamic state of a structure. However simple or more complex control unit depending on the nature of the problem been analysed might be required but, the basic idea is to have a fast efficient and cost effective system.

1.7.2 Methods used for SHM

The conventional method used for structural testing and health monitoring is known as Non Destructive Testing or Non Destructive Evaluation (NDT & NDE). This method involves the use of measuring techniques to inspect materials, structures and systems. Different measurement techniques are employed in NDT. Some of them can be identified here such as: visual inspection, strain gauges, Infrared Thermography (IRT), ultrasonic imaging, X-Ray radiography and optical lasers.

Visual inspection is a form of NDT done by eye examination over the structure using static optical or scanning electron microscope. Visual inspection is perhaps the simplest and least expensive method in a health monitoring process. Often, damage such as those typically found in composite structures tend to occur within the fibers of the material so it is not easy to identify them. In such circumstances eye observation would not be advantageous. However, this method can provide some useful data for large surface damage.

Strain gauge methods are one of the most common ways used for structural analysis. They allow the measurement of strain levels due to deformation. The gauges are usually in a form of a foil and work in a similar way to piezoelectric sensors except that their response to dynamic loading and other properties such as sensitivity, impedance and bandwidth differs quite significantly. These devices are relatively small, light and inexpensive making them simple to implement, and their results are easily interpreted. However some limitations of strain gauges include resolution and sensitivity which is required in monitoring applications.

Infrared Thermography (IRT) is a method for measuring the temperature distribution of a material surface. It permits the detection of regions of heat production (e.g. due to a crack under cyclic loading or a hot spot) or regions of cooling (e.g. due to blisters or air voids). IR thermography can be used to control the temperature of single components such as in the building phase of road construction (Baskar et al, 2006).

Ultrasonic imaging can be used to detect the location of damages such as cracks, pores, inclusions and flaws based on ultrasound waves. These waves are produced from a transducer which is connected to a diagnostic machine. This method is normally used for testing metal, ceramic and plastic materials. There are two methods of receiving the ultrasound waveform: reflection and attenuation. In reflection (or pulse-echo) mode, the transducer performs both the sending and the receiving of the pulsed waves as the "sound" is reflected back to the device. Reflected ultrasound comes from an interface, such as the back wall of the object or from an imperfection within the object. The diagnostic machine displays these results in the form of a signal with an amplitude representing the intensity of the reflection. However the equipment is expensive and access to the whole structure is required. Therefore parts must be disassembled for testing (Kessler, 2002).

X- Ray radiographic techniques rely on recording the difference in x-ray absorption rates through the surface of a structure. In other words it takes static radiographs of

the interior part of a structure where areas of different density are differentiated by the magnitude of the x-ray in a predetermined excitation time. To precisely detect damaged regions with cracks or delamination, often a liquid penatrant is applied to the area to be examined.

Optical laser methods consist of the use of embedded small diameter optical fibers which can be multiplexed to record strain measurements over large regions. When using this method of detection, pulses of polarized laser light are transmitted along an optical fiber, and gratings are placed in various locations to reflect a portion of the light at a certain wavelength. By recording the time of flight of the beam, the length of that segment of fiber can be easily deduced; if a strain has been applied to that segment of fiber, the time of flight would change.

These methods have been used quite extensively in structural monitoring. However, they require that the area to be inspected needs to be known a priori as well as be accessible in order to successfully monitor the structure i.e. for defects or damage.

Another important method of SHM is the Vibration-based method. The basic idea of vibration-based SHM is that damage will alter the stiffness, mass, or energy dissipation (damping) properties of the system which will result in changes in the dynamic response of the system. This type of method uses the response of the system to its natural operating conditions. In other words, it excites the structure to its fundamental or resonant frequency to observe its behaviour. This method is considered practical and reliable since any point in the structure can be selected to obtain the frequency information (Frederic, 1997). The structure can be excited by an external source (e.g. shaker) or a built–in source (e.g. piezoelectric actuator) and its response can be measured using a sensing device.

Using smart materials such as piezoelectric and piezoceramic for SHM has several advantages over traditional inspection methods. A built-in continuous system with sensors and actuators which are non-invasive can be introduced in the structural material during its manufacturing process. In this way, the structure can be monitored in real time and in situations were damages or defects tend to develop, their initiation and propagation can be detected at early stages and the necessary intervention taken (Chen & Wang, 2004).

1.7.3 Objectives of SHM Process

The goal of structural health monitoring is to ensure that the safety of a structure is maintained during its operational period. Structural health monitoring practices have relied and still rely on the use of conventional methods. With the new developments in materials science and technology, the primary objective of SHM is to be able to replace conventional testing techniques with continuous monitoring systems to provide real time information about the physical state of the structure being analysed. As stated by Kessler (2002), when using an ideal in-situ structural health monitoring system, components would remain in operation without regularly scheduled maintenance until the SHM system reported that a repair is necessary. For this reason, the entire network that makes up the system need to interact effectively to ensure reliable results are obtained. A schematic representation of structural health monitoring objectives is summarized in figure 4.3.

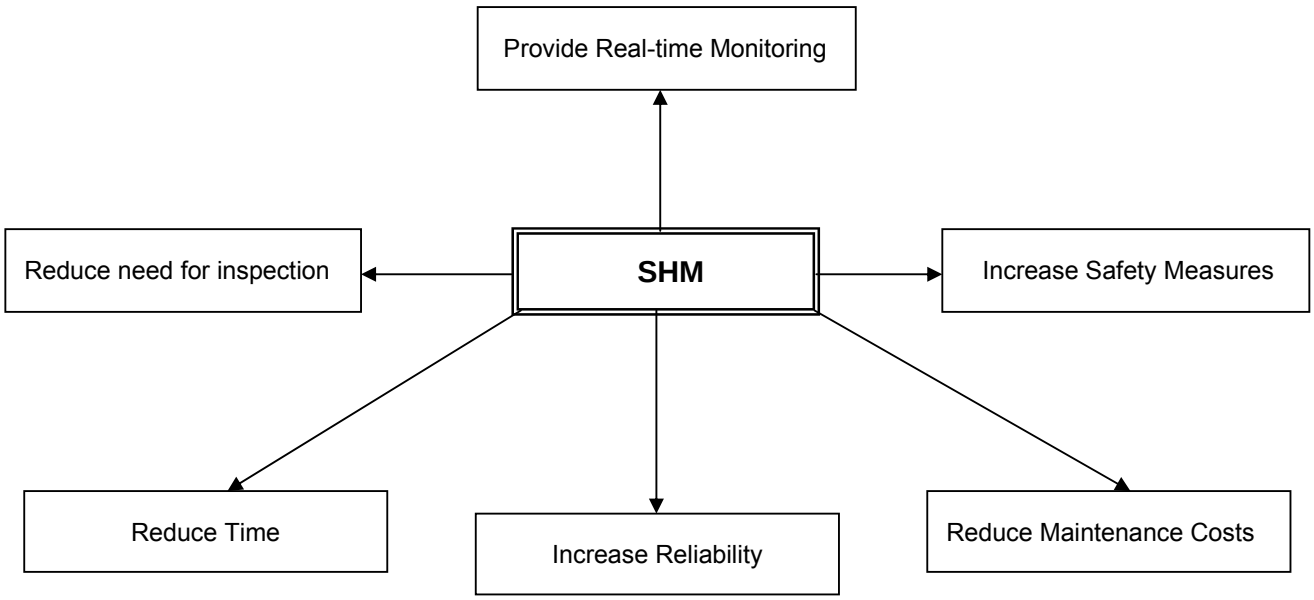

Fig 1.3: SHM objectives diagram

Another aspect of SHM technology is to employ systems with minimum labour involvement. The method using smart sensors and actuators has enormous potential for applications in monitoring aerospace, automotive, marine and other engineering structures and systems subject to fatigue, corrosion, impacts, shear or any other structural damage (Baskar et al, 2006).

Therefore, to be able to use these systems with confidence and ensure they are reliable, research still needs to be conducted to assess the capabilities of systems to facilitate the inspection analysis and interpretation of the physical condition of structures and components. Table 1.1 below summarises the advantages and disadvantages and well as potential of some methods used for SHM.

Table 1.1: Summary of SHM system capabilities

Method	Advantages	Disadvantages	SHM Potential
Visual	Inexpensive equipment Simple procedure Simple to implement	Only surface damage Only large areas No data analysis	Currently none
X-Ray Radiography	Capable of Internal damage detention Permanent record of results Simple Procedure	Expensive equipment Expensive to implement Can be time consuming Require skills for correct interpretation	Detention of internal damage growth and propagation
Strain gauge	Surface mounted Portable Simple procedure	Expensive equipment Expensive to implement	Light weight Low power required for operation
Optical Fibers	Inexpensive equipment Provide quick scan of large area	Must be embedded Requires laser in diagnostic process Expensive to implement	Light weight Can cover large areas
Ultrasonic	Portable Sensitive to small damage Quick scan of large area	Very expensive equipment Complex results Specialised system for operation	Detention of damage location based on ultrasonic waves

Vibration based	Inexpensive equipment Inexpensive to implement Simple procedure Portable Quick scan of large area	Requires specialised software in some cases High data rates	Lightweight Low power required Multi-purpose sensors and actuators Results for small and large areas

CHAPTER TWO

LITERATURE REVIEW ON PIEZOELECTRIC MATERIALS

2.1 Introduction

During the last decades, piezoelectric materials made huge contributions in technological and industrial fields. A significant amount of research has been directed towards the application of these materials for monitoring and control of structures and systems. Piezoelectric devices (made from piezoelectric materials) fit in to four general categories depending on what type of physical effect is aimed for. These categories are: sensors, actuators, generators and transducers. Sensors and generators make use of the direct piezoelectric effect. Actuators make use of the inverse piezoelectric effect and transducers used both effects with in the same device.

This chapter is focused on the theory of piezoelectric materials with main emphasis to Polyvinylidene Fluoride (PVDF) as a sensor. Furthermore, its formation, constitutive relations, properties, sensor production and attachment into composite structures is presented.

2.1.1 History of *Piezoelectricity*

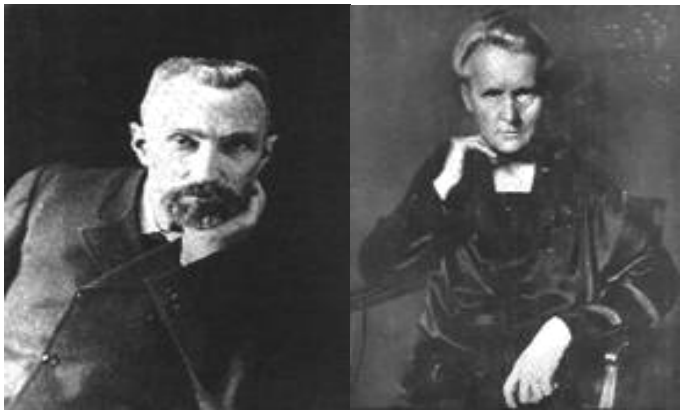

Fig 2.1 Pierre and Jacques Curie, 1880 (Piezoelectric History, 2005 Micromechatronics Inc)

Piezoelectricity was discovered around the 18th century by the two Franchmen brothers, Pierre and Jacques Curie. The Curie brothers observed that certain crystals

such as quartz had the ability to generate an electrical charge when mechanically stressed (Bar – Cohen & Lih, 1996). This was called the direct piezoelectric effect. The word piezoelectricity originated from the Greek word “piezeon”, which means to press or squeeze. The Curie brothers published their first experimental demonstration on piezoelectric activity in 1880. The experiment consisted of measurements of surface charges appearing on specially prepared crystals (tourmaline, quartz and Rochelle salt) which were subjected to mechanical stress.

However, they did not predict that the crystals would also exhibit the converse piezoelectric effect (strain or deform in response to applied electrical field). This property was mathematically deduced from fundamental thermodynamic principles by the physicist Gabriel Lippmann in 1881.

One of the first applications of this property was made in the 1920's by another Frenchman Langevin, who developed a quartz transmitter and receiver for underwater sound - the first SONAR before World War II (Harrison, 2001).Years later, in 1969, Kawai found very high piezo-activity in the polarized fluoropolymer, polyvinylidene fluoride (PVDF). The investigations conducted by Kawai were considered of significant importance as the material demonstrated not only strong chemical composition but also other properties such as lightweight, high flexibility and sensitivity, which could be used for many applications in the scientific and technological fields.

2.2 Piezoelectric Materials and Systems

Piezoelectric materials have been used in many different fields because of their special and attractive properties. In the development of intelligent structural systems, piezoelectric materials are been widely used as sensors and actuators for monitoring and control of static and dynamic structural conditions. Examples include the work of Vodicka and Galea (1998), who reported the use of PVDF sensors to monitor a wing pivot fitting doubler. The sensors were bonded to the wing pivot and tested under hot/wet conditions for a series of load cases. Good durability of PVDF and correlation was found when compared to conventional electrical resistance strain gauges. Analytical models for Distributed piezoelectric actuators (DPA) with complex shapes (T, L and Z shape) made of Lead Zirconate Titanate (PZT) were investigated by Sun and Qiu (2004). DPA essentially consisted of a solid state type of actuator that can be embedded in a structure and controlled by electrical signals with high bandwidth

and high precision. The investigation served to establish actuators with multidirectional functions for MEMS applications.

Shirinov and Schomburg (2007) developed a low cost pressure sensor for use in pneumatic and hydraulic systems. The sensor was tested under different media such as strong acids, alkalis and solvents to determine its chemical resistance. Experimental results have shown that the sensor is suitable to work in different environments although factors such as temperature, pressure, humidity and creep influenced the measurement accuracy.

2.3 Source of Piezoelectric Effect: Polarization

Polarization (*P)* is defined as a measure of the degree of piezoelectricity in a given material. In a piezoelectric material, a change in polarization results from an applied stress or strain under the conditions of constant temperature and zero electric field. A linear relationship exists between polarization and the piezoelectric constants governing the material's behaviour.

Piezoelectric materials are normally permanently polarized. This means that the molecules within the material have both positive and negative charges. The dipoles of these piezoelectric materials are facing in random directions. When an electric field is applied across them, the dipoles align themselves in the direction of the applied electric field causing the material to deform. Conversely when the material is mechanically deformed, the positive and negative charge centers displace by different amounts causing an electrical polarization within the crystal structure which generates a charge. Figure 2.1 below shows the unpolarised and polarised stages of a typical piezoelectric material, Lead Zirconate Titanate (PZT).

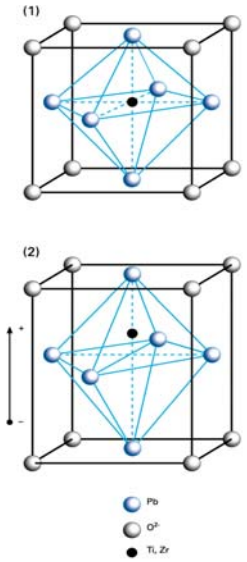

Figure 2.2: Polarised and unpolarised forms of PZT (Washington, 2002)

In the case of polymers such as PVDF the source of piezoelectricity is a dipole created by Fluorine and Carbon bonded in its structure. PVDF is half crystalline and half amorphous. The crystalline form consists of a non-polar alpha phase and a highly polar beta phase. The alpha phase is a non-polar phase, whereas the beta phase has the hydrogen and fluorine atoms arranged to give maximum dipole moment per unit cell (Bar – Cohen & Lih, 1996). These dipole moments are randomly oriented throughout the polymer chain creating polarization.

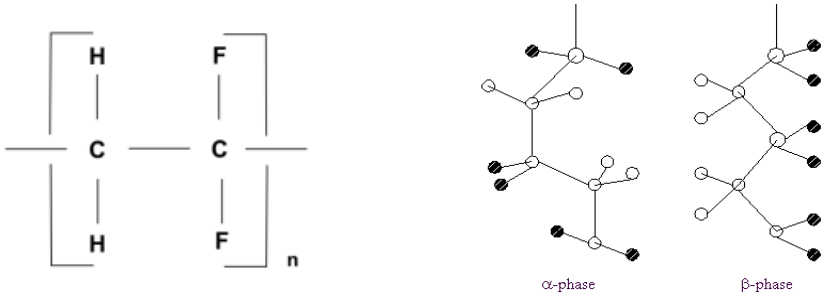

Fig 2.3: Chemical structure and polarization phase of PVDF (Huang, 1998)

The piezoelectric effect is anisotropic, meaning that it can only be exhibited by materials whose crystal structure has no centre of symmetry (Preumont, 1997). In this phase, the crystal has a built in electric dipole, but the net electric dipole on the macroscopic scale is zero. When the crystal is cooled in the presence of an electric field, the dipoles tend to align. After removal of the poling field, the dipoles can not return to their original position and the ceramic body becomes permanently

piezoelectric, with the ability to convert mechanical energy to electrical and vice versa. The direction of expansion with respect to the direction of electrical field depends on the constants appearing in the constitutive equations.

2.4 Piezoelectric Constitutive Equations

Piezoelectricity is described mathematically within a material constitutive equation, which defines how the piezoelectric displacement (D), electric field (E) stress (T) and strain (S) are related. According to Preumont (1997), "in an unstressed one-dimensional dielectric medium, the displacement *D* (charge per unit area, expressed in coulomb/m^2), is related to the electric field *E* (V/m) by":

$$D = \varepsilon \cdot E$$

Where ε is the permittivity of the material. Similarly, in a one-dimensional elastic body placed in a zero electric field, the strain *S* and the Stress *T* (N/m^2) are related by:

$$S = s \cdot T$$

Where *s* is the compliance of the material (inverse of Young's modulus). For a piezoelectric material, the electrical and mechanical constitutive equations can be expressed as:

$$S = s^E \cdot T + d \cdot E \tag{2.1}$$

$$D = d \cdot T + \varepsilon^T \cdot E \tag{2.2}$$

In equation (2.1), the piezoelectric constant (*d)* relates the strain to the electric field (*E)* in the absence of the mechanical stress and (s^E*)* refers to the compliance when the electric field is constant. Also in equation (2.2), (*d)* relates the electric charge per unit area (*D)* to the stress under a zero electric field; (*d)* and (ε^T) is the permittivity under constant stress (transpose of ε). The above equations give the strain-charge form. These equations can be transformed into:

$$T = \frac{1}{s^E} S - \frac{d}{s^E} E$$

$$D = \frac{d}{s^E} S + \varepsilon^T \left(1 - \frac{d^2}{s^E \varepsilon^T} \right) E$$

This gives the stress-charge forms which are usually rewritten as:

$$T = c^E S - eE \tag{2.3}$$

$$D = eS + \varepsilon^T \left(1 - k^2\right)E \tag{2.4}$$

Where

$c^E = 1/s^E$ is the young modulus under constant electric field (in N/m^2);

$e = d/ s^E$ is the constant relating the charge per unit area to the strain (in coulomb/m^2).

$k^2 = d^2/(s^E\varepsilon^T)$ is the coupling coefficient of the piezoelectric material. The coupling coefficient originates from the fact that at frequencies below the mechanical resonant frequency of the piezoelectric material k^2 is quite low and can be expressed as:

$$k^2 = \frac{stored\ energy\ converted}{Stored\ input\ energy}$$

Normally, a high k value is needed for an efficient material transduction. Equation (2.3) is used for the formulation of a piezoelectric laminar actuator and equation (2.4) for a piezoelectric laminar sensor. In matrix form this equations can be written as:

$$\begin{pmatrix} T \\ D \end{pmatrix} = \begin{pmatrix} c^E & -e \\ e & \varepsilon^s \end{pmatrix} \begin{pmatrix} S \\ E \end{pmatrix} \tag{2.5}$$

The above constitutive equations keep more or less the same form for multidimensional media with only exception that tensor quantities are involved. Thus, the strain-charge form (from equation 2.1 and 2.2) can be represented in a matrix form as:

$$\begin{bmatrix} S_1 \\ S_2 \\ S_3 \\ S_4 \\ S_5 \\ S_6 \end{bmatrix} \begin{bmatrix} d_{11} & d_{12} & d_{13} \\ d_{21} & d_{22} & d_{23} \\ d_{31} & d_{32} & d_{33} \\ d_{41} & d_{42} & d_{43} \\ d_{51} & d_{52} & d_{53} \\ d_{61} & d_{62} & d_{63} \end{bmatrix} \begin{bmatrix} E_1 \\ E_2 \\ E_3 \end{bmatrix} \begin{bmatrix} S_{11}^E & S_{12}^E & S_{13}^E & S_{14}^E & S_{15}^E & S_{16}^E \\ S_{21}^E & S_{22}^E & S_{23}^E & S_{24}^E & S_{25}^E & S_{26}^E \\ S_{31}^E & S_{32}^E & S_{33}^E & S_{34}^E & S_{35}^E & S_{36}^E \\ S_{41}^E & S_{42}^E & S_{43}^E & S_{44}^E & S_{45}^E & S_{46}^E \\ S_{51}^E & S_{52}^E & S_{53}^E & S_{54}^E & S_{55}^E & S_{56}^E \\ S_{61}^E & S_{62}^E & S_{63}^E & S_{64}^E & S_{65}^E & S_{66}^E \end{bmatrix} \begin{bmatrix} X_1 \\ X_2 \\ X_3 \\ X_4 \\ X_5 \\ X_6 \end{bmatrix} \tag{2.6}$$

$$\begin{bmatrix} D_1 \\ D_2 \\ D_3 \end{bmatrix} \begin{bmatrix} T_{11} & T_{12} & T_{13} \\ T_{21} & T_{22} & T_{23} \\ T_{31} & T_{32} & T_{33} \end{bmatrix} \begin{bmatrix} E_1 \\ E_2 \\ E_3 \end{bmatrix} \begin{bmatrix} d_{11} & d_{12} & d_{13} & d_{14} & d_{15} & d_{16} \\ d_{21} & d_{22} & d_{23} & d_{24} & d_{25} & d_{26} \\ d_{31} & d_{32} & d_{33} & d_{34} & d_{35} & d_{36} \end{bmatrix} \begin{bmatrix} X_1 \\ X_2 \\ X_3 \\ X_4 \\ X_5 \\ X_6 \end{bmatrix} \tag{2.7}$$

Matrix (2.6) describes the direct piezoelectric effect and (2.7) the converse effect. Piezoelectricity, is a cross coupling between the elastic variables: stress (*X* or *T* subscripts are normally used) with 6 elements, strain (*S)* with 36 elements, and the dielectric variables: electric charge density (*D)* and electric field (*E)* each with 3 elements. These elements are considered due to the anisotropic nature of piezoelectric materials. Their mechanical and electrical behaviour depend upon the direction of external applied mechanical/electrical field relative to a set of fixed axis in the material. However it is worth mentioning that the mechanical stiffness of certain piezoelectric materials such as PVDF is usually much smaller compared to the structure they are attached to due to their high flexibility. Therefore the anisotropic behaviour can be neglected and only the direction of applied mechanical stress/voltage (which is normally the longitudinal axis) is considered as seen in equation 2.3 and 2.4

2.5 Properties of Piezoelectric Materials

2.5.1 Directions and Constants

In order to define the electro-mechanical properties of piezoelectric materials, conventions have been established based on coordinate system notation (as shown in Figure 2.4). The stretch direction is denoted by axis 1 (along the length). Axis 2 is orthogonal to the stretch direction in the plane of the material (through the width). The polarization axis perpendicular to the surface of the material is denoted as 3 (thickness axis). The shear planes are indicated by the subscripts 4, 5, 6 and are perpendicular to the directions 1, 2, and 3 respectively.

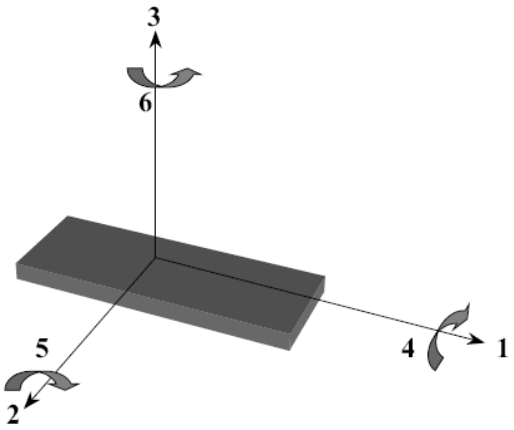

Fig 2.4: Conventional directions for piezoelectric materials (Harrison, 2001)

The piezoelectric constants are interrelated through the electrical and mechanical properties of the material. Electric field strength and electric charge density are related through the dielectric constant, (where ε is the permittivity of free space), while stress and strain are related through the compliance according to (Harrison, 2001):

$d_{ij} \quad o_i g_{ij}$

$e_{ij} \quad s_{ij} d_{ij}$

Where:

d_{ij} - Strain coefficient or charge output coefficient

The strain developed [m/m] per unit of electric field strength applied [V/m] or (due to the sensor / actuator properties) charge density developed [C/m2] per given stress [N/m2].

g_{ij} - Voltage coefficient or field output coefficient

The open-circuit electric field developed [V/m] per applied mechanical stress [N / m^2] or (due to the sensor / actuator properties) strain developed [m/m] per applied charge
density [C/m^2].

e_{ij} - Dielectric Coefficient

The dielectric constant which consists of the coupling coefficient k_{ij} (dimensionless) divided by the voltage coefficient g_{ij} [C / m^2]

For a coefficient, d_{ij}, the first subscript is the direction of the electric field or charge displacement while the second subscript gives the direction of the mechanical deformation or stress.This relates the amount of charge generated on the surfaces of the material on the *i*-axis to the force applied on the *j*-axis. For example if a force *F* is applied (in the poling direction) to a rectangular block containing a piezoelectric film (i.e. PVDF) with electrodes on both sides, the charge generated is given by:

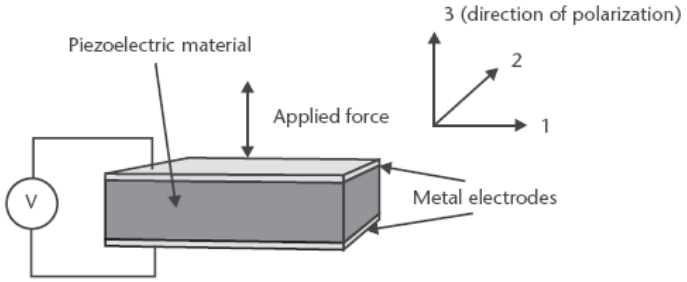

Fig 2.5: Applied force resulting in voltage generation

$$Q = d_{33}F_3 \tag{2.8}$$

The presence of charge (*Q*) in the metallized electrodes produces a potential difference across the block which can be expressed as:

$$V = \frac{Q_3}{C} = \frac{d_{33}F_3 t}{\varepsilon_0 \varepsilon_r A} \tag{2.9}$$

Where *C* represents the capacitance of the material, ε_0 is the permittivity of free space ε_r the relative permittivity, *A* is the area of the block and *t* the thickness of the piezoelectric material.

Coefficient g_{ij}, i gives the direction of applied mechanical stress and *j* the strain per applied charge. For e_{ij}, i gives the direction of applied mechanical stress which develops strain per applied charge (since k is dimensionless). However, one of the most important electromechanical properties to consider for the purpose of this work is the dielectric coefficient *e* which consists of the electromechanical coupling factor *k* and the stress constant *g*. A high coupling factor would give a greater sensitivity to the piezoelectric material in converting applied mechanical stress into an electrical signal. Table 2.1 shows the typical properties of piezoelectric materials.

Table 2.1: Typical properties of piezoelectric materials (Piezo Films, 2006)

Property	Units	PVDF	PZT	$BaTi0_3$
Density	10^3kg/m³	1.78	7.5	5.7
Relative Permitivity	$\varepsilon/\varepsilon_o$	12	1200	1700
d_{31} constant	10^{-12}C/N	23	110	78
g_{31} constant	10^{-3}Vm/N	216	10	5
k_{31} constant	% at 1 KHZ	12	30	21
Acoustic impedance	106kg/m²-sec	2.7	30	30

2.5.2 Pyroelectricity and Ferroelectricity

Pyroelectricity is a subgroup of piezoelectric materials that form permanent dipoles and develop polarization. This polarization changes with temperature. In other words, these materials are also temperature dependent. As they absorb thermal energy, they expand or contract, thereby inducing secondary piezoelectric signals. When a piezoelectric film is heated, the dipoles within the film exhibit random motion by thermal agitation. This cause a reduction in the average polarization of the film, generating a charge build up on the film's surface. The output current is proportional to the rate of temperature change (ΔT). The amount of electrical charge produced per degree of temperature increase or decrease is described by the pyroelectric charge coefficient (*p*), and the temperature change in a given area (*A),* (Piezo Films, 2006).

$$Q = p\Delta TA \tag{2.10}$$

Equally, the voltage produced is a function of the pyroelectric charge coefficient, temperature change (ΔT), thickness (*t)* and permittivity (ε). Therefore:

$$V = \frac{pt\Delta T}{\varepsilon} \tag{2.11}$$

Piezoelectric materials are also ferroelectric. Ferroelectricity is a physical property of the material to exhibit spontaneous electric dipole moment. At high electric fields, the polarization that occurs in semicrystalline polymers such as PVDF is nonlinear with

the applied electric field. This nonlinearity in polarization is defined as hysteresis. Figure 2.4 is an example of the typical hysterisis behaviour of PVDF. Two other important properties of ferroelectric polymers are the coercive field and the remanent polarization. The coercive field, E_c, which marks the point where the hysterisis intersects with the horizontal axis, is typically about 50 MV/m at room temperature for many ferroelectric polymers (Harrison, 2001).

The remanent polarization, P_r, corresponds to the point where the loop intersects with the vertical axis. The values of *Ec* and *Pr* are dependent on the temperature and frequency of measurement. The Curie temperature T_c, is generally lower than but close to the melting temperature of the polymer. Below T_c, the polymer is ferroelectric and above T_c the polymer loses its piezoelectric effect.

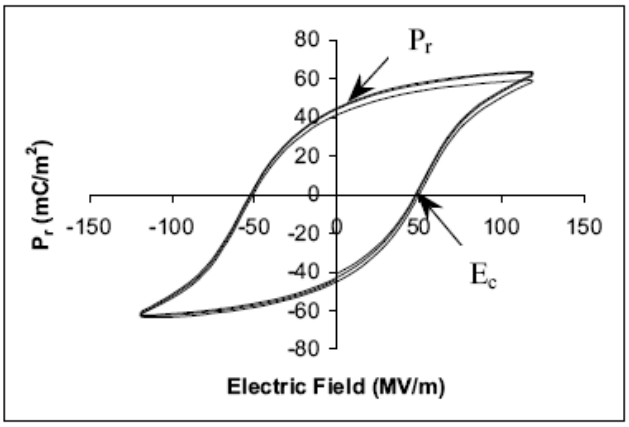

Fig 2.6: Typical hysterisis loop for PVDF (Harrison, 2001)

2.6 Production Process of PVDF Films

Polyvinylidene fluoride is not piezoelectric in its raw state, but can be made piezoelectric by heating the PVDF within an electric field. The production typically starts with the melting and extrusion of resin pellets into the form of a sheet. This operation is followed by further stretching the sheet, at a temperature below the melting point, to obtain the beta-phase polymer (strong poling).The beta-phase polymer demonstrates high levels of piezoelectricity when exposed to an appropriate electric field (Piezo Films, 2006).

Under the exposure of the electric field, the crystallites realign in a direction relative to the applied electric field. The copolymers of PVDF are polarised without stretching.

The films are then coated with an electrically conductive silver or gold layer made of copper or nickel, which serves as electrodes on both sides of the film to provide a conducting surface. Following this step, the films are laminated with protective layers, cut to proper sizes, and packaged. PVDF films are usually produced in a clean room environment to ensure the films do not get contaminated by any external source. The final product is a thin, flexible, lightweight, and tough film which can be used as a sensor (Luo & Hanagud, 1999). Typically, the thickness of PVF films appropriate for MEMS are given in standard values varying from 9 to 220 μm. The voltage generated by the sensor when mechanically stressed is collected by the conductive coating on both sides of the film.

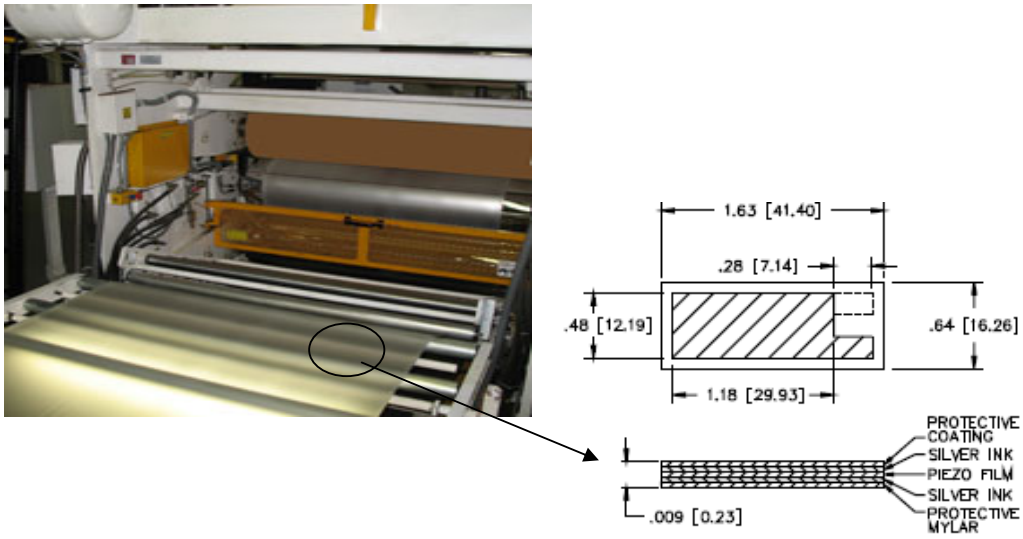

Fig 2.7: Characteristics of a typical PVDF film (Piezo Films, 2006)

2.6.1 Material Properties

Some of the main properties of the PVDF material after processed are (Piezo films, 2006):

- Good mechanical strength: PVDF although flexible is a tough material which can withstand external loading

- Resistant to chemicals and low impedance: It performs quite well in harsh environments when exposed to acid and alkaline solutions and has low acoustic impedance close to that of water, human tissue and some organic materials which is essential for medical and underwater applications

(Piezoelectric Systems, Inc).

- Require no power to operate: Because of its piezoelectric property PVDF is a self charge material.

- Inexpensive: The films are manufactured at low cost in thin sheets of different thicknesses.

- Low density and excellent sensitivity: the compliance of the films is 10 times greater than the compliance of ceramic materials. The sensitivity of PVDF film as a receiver of mechanical work input is quite high. In its simplest mode the film behaves like a dynamic strain gage except that it requires no external power source and generates signals greater than those from conventional foil strain gauges after amplification.

2.7 Sensor Fabrication Methods

PVDF films manufactured in sheets can be cut to the required size and shape relevant for an application and lead wires are attached to translate the signals produced. There are different methods to make an effective sensor from a PVDF film. The difference in most methods resides on the way in which lead wires are attached to the film. Some of these methods briefly discussed here are (Piezo Films, 2006):

2.7.1 Coat Etching Method

This method consists in removing part of the conductive silver/gold coating on both sides of the film. This can be achieved by etching the silver ink with a cotton bud soaked solvent such as Methyl Ethyl Ketone (Vodicka and Galea, 1998). This creates attachment tabs for wire connections and prevents the electrodes from short circuiting at the joining area. The etching also allows a precisely defined active sensing area.

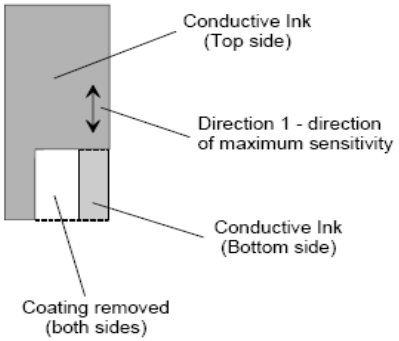

Fig 2.8: Etching of conductive coating to create an effective sensor (Piezo Films, 2006)

Once etched, crimp connecters with solder tabs for fixing wires can be used or the crimp ends can be inserted into corresponding holes in a Printed Circuit Board (PCB) and soldered to the underside. Crimps are normally designed to work for a specified thickness of substrate and therefore the film may require padding on one side i.e. Polyester reinforcement to accommodate the crimp connecters. The clinches can be crimped on the upper and lower parts of the PVDF to ensure solid electrical and mechanical contact before attaching to the wire circuit leads.

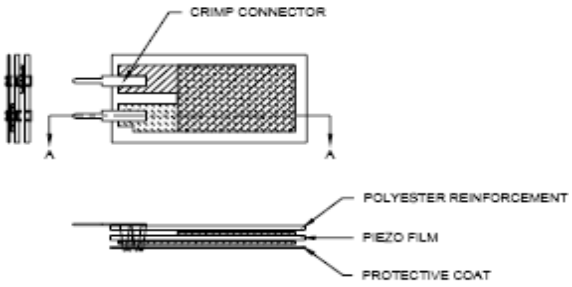

Fig 2.9: PVDF film sensor with crimp connector (Piezo Films, 2006)

2.7.2 Conductive epoxy Method

This method also requires etching of the silver ink. The lead wire connection is made using conductive epoxy which consists of epoxy and hardener mixture. After mixing properly, the combination can be used to attach the wires directly to the PVDF film on the connection tabs which have been etched providing a permanent connection. The epoxy can be cured at room temperature but curing time can be accelerated with higher temperatures. Mechanical clamping to hold the wires in place while curing is

required. However, both methods explained above require careful attention when etching the silver ink to ensure it does not affect other parts of the film either than the one selected. Once other areas are affected the film is depolarised.

2.7.3 Copper foil tape Method

Another method which does not require etching of the PVDF film conductive ink is using a copper foil tape to connect the lead wires. This is done by cutting a small piece of copper foil tape and then soldering the lead wires onto the copper foil before sticking it to either side of the PVDF film. This is to avoid high soldering temperatures from degrading the PVDF film. The tape being used must have an electrically conductive adhesive so that the lead wire can conduct the signals produce by the sensor.

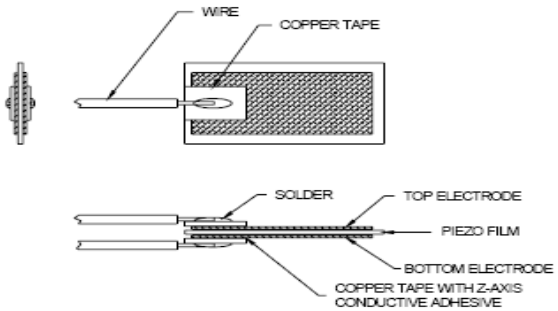

Fig 2.10: Copper tape attachment (Piezo Films, 2006)

2.8 Sensor Embedding Techniques and Material Integrity

In the study of structural health monitoring, piezoelectric sensors are normally bonded to the surface of the structure or embedded inside it. The embedding method requires special attention because of the structure's integrity and sensor's functionality which have to be preserved. Problems that may typically arise prior to embedment include sensor malfunctioning, reduction in the load carrying capacity (defects) of the structure and others depending on the type of structure and embedding method. In the case of fibre reinforced matrix composite structures, the sensor has to withstand the composite curing temperature without significant degradation and provide good bond to the substrate. A composite structure is a structure that has more than one constituent material that differs in form and chemical composition. The main reason why composite materials are formed is to enhance the properties of a material for certain applications. These materials are normally characterised by high strength and low weight proving superiority to other

materials. There are two classification systems of composite materials. One of them is based on the matrix material (metal, ceramic, polymer) and the other is based on the material structure. Each one of them is divided in to subgroups (Theodore, 1998):

1. Matrix material based Composites

Metal Matrix Composites (MMC): Metal Matrix Composites are composed of a metallic matrix (aluminium, magnesium, iron, copper)and a dispersed ceramic (oxides, carbides) or metallic (lead, tungsten, molybdenum) phase.

Ceramic Matrix Composites (CMC): are composed of a ceramic matrix and embedded fibers of other ceramic materials (dispersed phase).

Polymer Matrix Composites (PMC): these are composed of a matrix from thermoset (Unsaturated Polyester UP), Epoxy Polyester EP) or thermoplastic (Polycarbonate (PC), Polyvinylchloride, Nylon, Polyesterene) and embedded glass, carbon, steel or kevlar fibers (dispersed)

2. Reinforcing material structure based Composites

Particulate Composites: consist of a matrix reinforced by a dispersed phase in form of particles. Dispersed phase of these materials consists of two-dimensional flat platelets (flakes), laid parallel to each other.

Fibrous Composites: Fibrous composite are classified in two parts:

Short-fiber reinforced composites. Short-fiber reinforced composites consist of a matrix reinforced by a dispersed phase in form of discontinuous fibers with random or preferred orientation.

Long-fiber reinforced composites consist of a matrix reinforced by a dispersed phase in form of continuous fibers. These can be presented as unidirectional orientated fibers or bidirectional oriented fibers (woven).

Laminate Composites: reinforced composite consisting of several layers with different fiber orientations, called multilayer (angle-ply) composite.

The embedding technique for the different composite materials mentioned above differs. Some composites such as the ones in the matrix material based category, the piezoelectric sensors/actuators can be embedded or sandwiched between the layers

of the composite using adequate bond adhesives. This process normally takes place at room temperature and compatibility between the type of composite and sensor must exist to ensure proper bonding. Improper bonding would result in damage such as debonding or separation of both parts which could affect sensor functionality and structural integrity.

For the reinforced material based category, the sensors/actuators can be embedded during the manufacturing process of the composite. This process can take place either at room or higher temperatures depending on the specific method used. Typical methods include vacuum bagging, vacuum infusion and resin to matrix transfer which have different composite curing approaches. Researchers have proposed methods to embed piezoelectric sensors in these composites to assess their effect on the structure integrity. Yang et al (2005) developed a smart layer composed of single side flexible polyimide film sensor and embedded in to a carbon fibre composite plate.

Pan, Liang & Li, 2006, proposed a method to embedded optical fiber sensors in a fiber glass composite structure. Their method consisted in integrating the optical sensors with a polyimide film as a layer and embed the layer in the structure.

Another method was proposed by Rye & Nemat-Nasser (2007). The method consisted of embedding sensors between the layers of prepreg glass epoxy composite material and precision punched cut-outs of the prepreg material.

The results obtained from these studies have shown good interaction between the sensor and the composite structure.

2.9 Sensor Response Measurement

When piezoelectric films of PVDF are used as sensors, two measurement conditions are usually possible. The first one consists in measuring the electric charge or the electric current generated by the material. The second possibility is to measure the electric potential between the electrodes of the piezoelectric sensor. In this case, the output voltage can be measured by connecting the electrodes of the piezoelectric sensor to a high input impedance device such as an oscilloscope or voltmeter through a probe. Once connections are made, an important property of the film to consider is its capacitance. Capacitance is a measure of any component's ability to store electrical charge and is always present when two conductive plates are brought

close together. For the PVDF film the conductive plates are represented by the conductive electrodes on both surfaces of the film. The capacitance of the film is strongly affected by the properties of the insulator serving to space the plates apart. The measure of the insulator's capacity to store charge is given by its dielectric constant or permittivity. The capacitance of the film will increase as its area increases. Therefore, a large sheet of film will have a larger capacitance than a small sheet. Capacitance also increases as the film thickness decreases. Therefore, for the same surface geometry, a thin film will have a higher capacitance than a thick film. These can be seen in the equation below:

$$C = \varepsilon \frac{A}{t} \tag{2.12}$$

Where:

ε represents the permittivity of the film (F/m)

A the cross sectional area (m^2)

t the thickness of the film (m)

CHAPTER THREE

BENDING DEFORMATION OF BEAMS EQUIPPED WITH SENSOR

3.1 Introduction

Beams represent the most common structural component found in civil and mechanical structures. Because of their vast application, they are extensively studied in Solid Mechanics and Strength of Materials courses, and in many cases are also used as a starting point to model complex structures. For instance, structures like helicopter rotor blades, airplane wings, spacecraft antennae, robot arms, flexible satellites, long-span bridges and subsystems can be modeled as a beam member (Malatkar, 2003). Therefore, studying the response of this simple structural component under different conditions would help in understanding and explaining the behavior of more complex real structures.

A beam is basically a bar designed to resist a combination of loading actions such as bending, transverse shears, axial stretching or compression, buckling and torsion. The bending action produces compressive longitudinal stresses in one side of the beam and tensile stresses on the other side. The two regions are separated by a neutral surface of zero stress, the neutral axis. The combination of tensile and compressive stresses in a beam produces an internal bending moment.

In this chapter, bending analysis of composite cantilever beams under static and dynamic conditions is presented. Derivations of the deformation and stress-strain state of beams with embedded thin piezoelectric film sensors is discussed.

3.2 Deformation of Smart Composite Beam

In the design of smart structures (structures with built in sensing or actuating capabilities or the combination of both) and MEMS systems, piezoelectric materials usually in the form of films are bonded or embedded to the structure which is to be monitored. Depending whether the piezoelectric film is to be used as a sensor or an actuator, the geometrical arrangement of the structure is made to coincide with that of the piezoelectric film. In other words, the strain coefficient of the piezoelectric material d_{31} dominate the design in the case of an actuator to excite the structure

along the longitudinal axis and d_{33} in the case of a sensor to sense the strains due to applied displacement (Preumont, 1997). In order to describe the response of a piezoelectric material when attached to a beam structure it is necessary to understand the principles of beam theory.

3.2.1 Derivation of Internal and External Bending Moments

Consider a cantilever beam with a thin and flexible strip of piezoelectric material embedded at a discrete location along its length. The piezoelectric strip is embedded near the top surface of the beam to maximize its effect. The thickness of the piezoelectric material (*h)* is assumed to be very small compared to the thickness (*H)* of the beam, *h* <<*H*. The beam is assumed to be uniform and homogeneous with cross section in the y-z plane. The piezoelectric material is placed at a distance *t* from its bottom surface to the neutral axis of the beam. The following further assumptions according to classical or Bernoulli beam theory can be made about the beam and piezoelectric material:

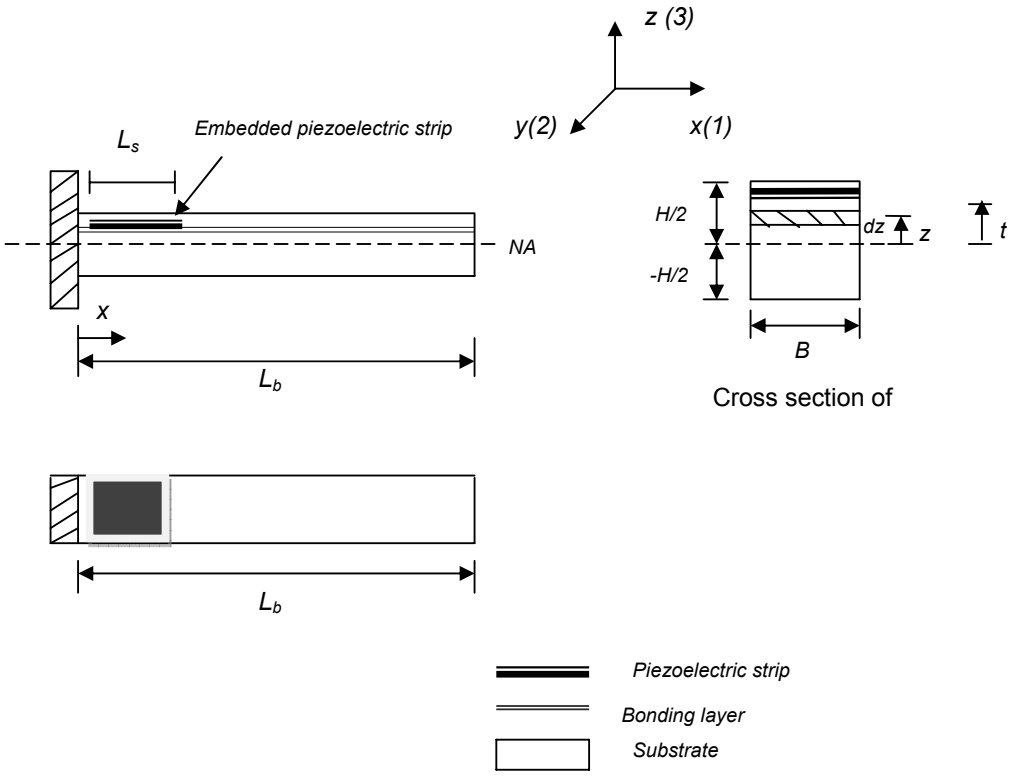

Fig 3.1: Beam with embedded piezoelectric film

- Long and thin (slender) beam – ratio of length to thickness and width greater than 20
- Loading is through the z-direction
- The beam undergoes small deflections and is made of a linear elastic material
- Plane sections originally normal to the longitudinal axis of the beam remain plane and normal to the deformed longitudinal axis upon bending
- Shear, axial forces or rotary inertia effects are neglected
- Perfect bond between the beam and piezoelectric strip
- The thickness of the bonding layer is neglected and there are no stress transfer between the beam and piezoelectric strip interface
- The local increase in stiffness of the beam due to sensor integration is neglected

Bending action creates moments on the beam. These moments can be internal due to beam geometry and material properties and external due to applied loading. An equation governing the beam under static condition may be written as (Srinivasan, 2001):

$$\frac{d^2}{dx^2}\left[M_0(x) - M_E(x)\right] = 0 \tag{3.1}$$

Where $M_0(x)$ is the beam internal moment about the neutral axis, and $M_E(x)$ is the moment due to external applied load. In order to understand the internal bending state of a beam we look at a segment of the beam and derive the moment equations.

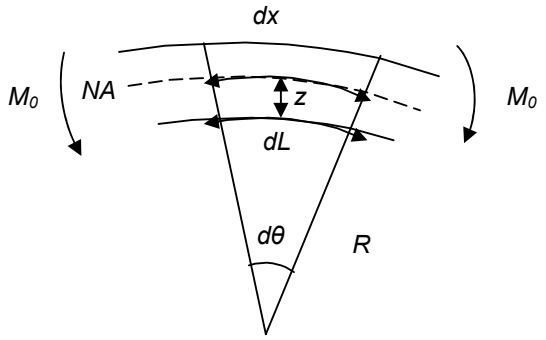

Figure 3.2: A differential segment of a beam in pure bending

The above figure shows a small section of the beam under pure bending. The length of the section at an arbitrary position is a function of *z*. By using the simple geometric definition of an arc length and subtended angle,

$$\theta = \frac{arc\ length}{radius} \tag{3.2}$$

Applying this relationship to both the neutral axis segment *dx* and compressed axis segment *dL* we find that

$$dx = R \cdot d\theta \tag{3.3}$$

$$dL = (R - z) \cdot d\theta \tag{3.4}$$

Solving for dθ in equation 3.3 and 3.4 gives:

$$d\theta = \frac{dL}{(R - z)} \tag{3.5}$$

$$d\theta = \frac{dx}{R} \tag{3.6}$$

Using equation 3.4 and 3.6 we find

$$dL = R \cdot d\theta - z \cdot d\theta \tag{3.7}$$

$$dL = dx - \left(\frac{z}{R}\right) \cdot dx \tag{3.8}$$

$$dL - dx = -\left(\frac{z}{R}\right) dx \tag{3.9}$$

$$\frac{dL - dx}{dx} = -\left(\frac{z}{R}\right) dx \tag{3.10}$$

The beam (Euler-Bernoulli) theory states that the neutral axis does not change in regardless of bending. Since the change in the segment length between the neutral axis and the compressed axis can be expressed as *dL-dx* and the original length can be expressed as dx we can conclude that *(dL-dx)/dx* is equivalent to the axial strain where:

$$\varepsilon_{axial} = \frac{\Delta L}{L} = \frac{dL - dx}{dx} = -\left(\frac{z}{R}\right) \cdot dx \tag{3.11}$$

For a beam under pure bending the internal moment M_0 is described as:

$$M_0(x) = \int_A \sigma_x z\, dA \tag{3.12}$$

$$\sigma_{xx} = E \cdot \varepsilon_{xx} = \left(\frac{E \cdot z}{R}\right) \cdot dx \ (\textit{from relations developed above})$$

$$dA = B \times dz$$

Where:

σ_{xx} is the stress in the outer fibers of the beam

E is the elastic modulus of the beam material

ε_{xx} is the axial strain in the beam

z is the distance from the element dz to the neutral axis of the beam

dA is the elemental area which is equal to the width multiply by the elemental thickness

Substituting in to the internal bending moment equation yields:

$$M_0(x) = \int_A E\frac{z^2}{R}dA = \frac{E\cdot B}{R}\int_{-\frac{H}{2}}^{\frac{H}{2}} z^2 dz = \left(\frac{B\cdot H^3}{12}\right)\frac{E}{R} \tag{3.13}$$

Where $BH^3/12$ represents the moment of inertia of a slender beam with rectangular cross section. For other cross sections it can be derived in a similar way depending on the position of the integrating variable with respect to the neutral axis. E represents the elastic modulus of the beam and piezoelectric material (since the piezoelectric strip is assumed to be small in size compared to the beam structure). Thus we find that the equation for a bending beam is given by:

$$\frac{1}{R} = \frac{M}{E\cdot I} \tag{3.14}$$

If the free end of the beam is subjected to a point load *P*, the beam will deflect into a curve. According to figure 3.3, the length of the differential beam segment is given by:

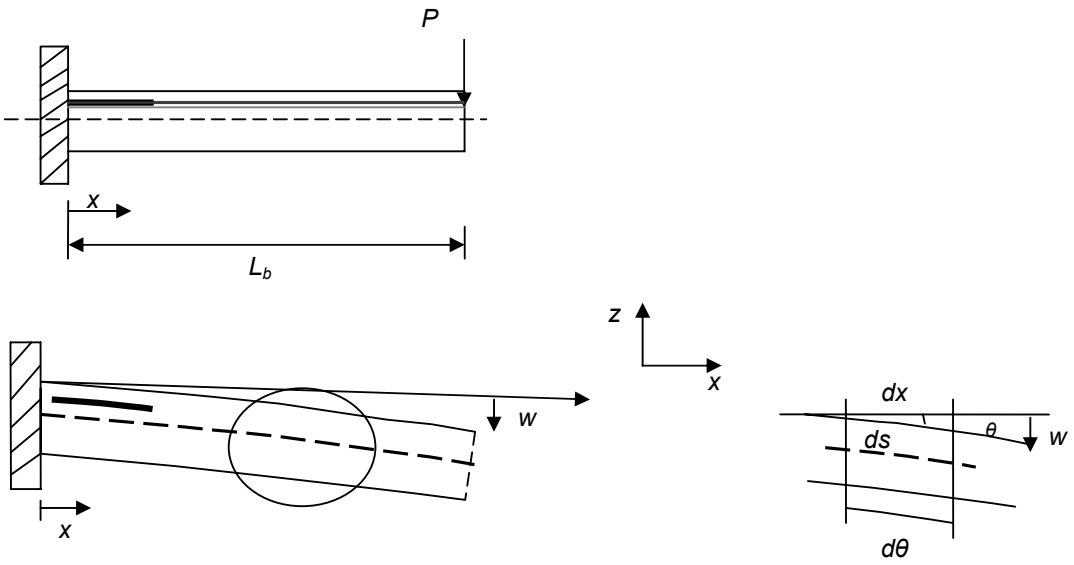

Fig 3.3 Cantilever beam with transversely applied load and Geometry coordinate system

$$ds = \frac{dx}{\cos\theta} \tag{3.15}$$

Where θ represents the angle of the beam with respect to the x-axis. The slope of the beam at any point is:

$$\frac{dw}{dx} = \tan\theta \tag{3.16}$$

From the previous section, we know that:

$$ds = R \cdot d\theta \tag{3.17}$$

Considering small-angle deflection, *ds*=*dx* and the following substitutions and simplifications can be made:

$$\frac{d\theta}{ds} = \frac{1}{R} \tag{3.18}$$

$$\frac{d\theta}{dx} \approx \frac{1}{R}$$

$$\tan\theta \approx \theta \tag{3.19}$$

$$\theta = \frac{dw}{dx}$$

By differentiating equation 3.19 we find:

$$\frac{d^2w}{dx^2} = \frac{d\theta}{dx} \tag{3.20}$$

Substituting the above equation in to equation 3.14 and 3.18 yields:

$$\frac{d^2w}{dx^2} = \frac{1}{R} = \left(\frac{M}{E \cdot R}\right)\frac{d\theta}{dx} = k_c \tag{3.21}$$

The above equation represents the bending curvature differential equation for small angle bending of slender beams. However, if *θ* becomes so large that small-angle approximations are invalid, a more exact expression for radius of curvature must be used. In this case :

$$\theta = arc\tan\frac{dw}{dx} \tag{3.22}$$

The derivative of an arc tan function is:

$$\frac{d\left(arc\tan u\right)}{du} = \frac{1}{1+u^2} \tag{3.23}$$

By taking the derivative of θ with respect to x we find:

$$\frac{d\theta}{dx} = \frac{\frac{d^2w}{dx^2}}{1+\left(\frac{dw}{dx}\right)^2} \tag{3.24}$$

Now using Pythagoras theorem we find that:

$$ds^2 = dx^2 + dw^2 \tag{3.25}$$

Dividing both sides by dx^2 yields:

$$\left(\frac{ds}{dx}\right)^2 = 1+\left(\frac{dw}{dx}\right)^2 \tag{3.26}$$

The above equation can be simplified to:

$$\frac{ds}{dx} = \sqrt{1+\left(\frac{dw}{dx}\right)^2} \tag{3.27}$$

With reciprocal

$$\frac{dx}{ds} = \sqrt{\frac{1}{1+\left(\frac{dw}{dx}\right)^2}} \tag{3.28}$$

By multiplying equation 3.24 by 3.28 we find:

$$\frac{d\theta}{ds} = \frac{d\theta}{ds}\cdot\frac{dx}{ds} = \frac{\frac{d^2w}{dx^2}}{1+\left(\frac{dw}{dx}\right)^2}\cdot\sqrt{\frac{1}{1+\left(\frac{dw}{dx}\right)^2}} \tag{3.29}$$

Substituting in to equation 3.21 gives:

$$\frac{1}{R} = \frac{\frac{d^2w}{dx_2}}{1+\left(\frac{dw}{dx}\right)^2}\cdot\sqrt{\frac{1}{1+\left(\frac{dw}{dx}\right)^2}} = \frac{\frac{d^2w}{dx^2}}{\left[1+\left(\frac{dw}{dx}\right)^2\right]^{\frac{3}{2}}} \tag{3.30}$$

The above equation provides an expression for the radius of curvature taking in to account large angle deflection. In order to derive the deflection equation for a cantilever beam with a load applied at its end and considering small deflections we can solve the second order linear equation (3.21). The following conditions apply:

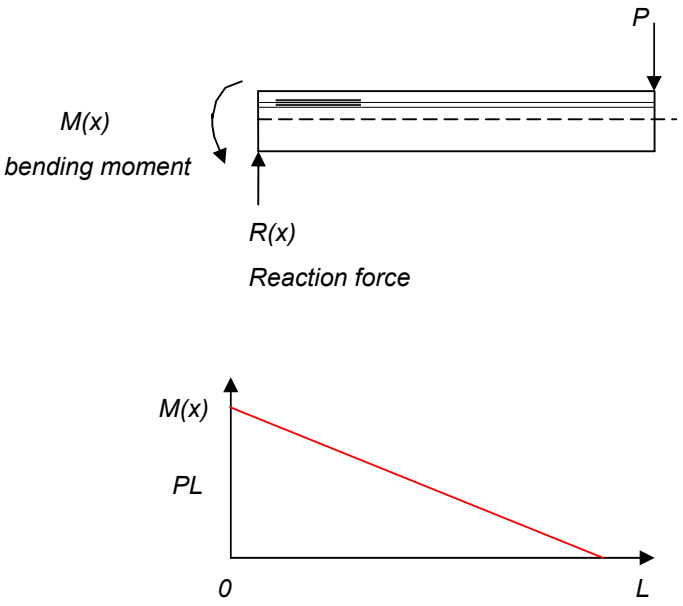

Fig 3.4 Free body and bending moment diagram of the beam

Equilibrium

$$\sum F_z = 0 \tag{3.31}$$

$$R(x) = -P \tag{3.32}$$

$$\sum M(x) = 0$$

The moment generated by this load is:

$$M(x) = -P(L_b - x) \tag{3.33}$$

Substituting equation 3.33 in to equation 3.14:

$$\frac{d^2 w}{dx^2} = \frac{-P(L_b - x)}{E I} \tag{3.34}$$

Since equation. 3.34 is a linear equation, we can solve it by assuming a solution of the form (Yee J, 2003):

$$w = A + Bx + Cx^2 + Dx^3 \tag{3.35}$$

Substituting in to the boundary equations for a cantilever:

$$\frac{dw}{dx}\Big|_{x=0} = 0 \tag{3.36}$$

$$w(0) = 0$$

Solving this system of equation we find that:

$$A = B = 0 \tag{3.37}$$

$$C = \frac{PL}{EI} \tag{3.38}$$

$$D = \frac{-P}{6EI} \tag{3.39}$$

Substituting in to equation 3.8 we obtain the deflection characteristic for a cantilever beam with point load, *P*

$$w = \frac{PL_b}{2EI} \cdot x^2 \cdot \left(1 - \frac{x}{3L}\right) \tag{3.40}$$

By setting x equal to L, the maximum deflection at the end of the cantilever beam is:

$$w_{\max} = \frac{PL_b^3}{3EI} \tag{3.41}$$

Note that the elastic modulus does not depend on the length of the beam structure. Furthermore, since it is a force *per* unit area (have units of N/m^2 or Pa) it does not depend on the cross-sectional area either. Thus elastic modulus is not dependent on the geometry of the structure, but only on the internal properties of the material. We can use the elastic modulus to predict how an object or structure of any size or shape will deform under a given load.

3.2.2 Strain-Stress State of Smart Composite Beam

Strain represents a change in the dimensional configuration of a body and stress a result of induced strain. Both quantities depend on a certain rate of applied loading and are important parameters in any compliant structure. When the beam equipped with a piezoelectric film sensor is bent by an external load *P* at its tip in to a downward curvature, the portion of the beam above the neutral axis and the top would be placed in tension and the bottom in compression. The strain is continuous at the beam-sensor interface. An assumption of perfect bonding is considered as previously mentioned which allows continuity of displacement at the interface of the beam layer and sensor. This means that if the structure is deformed by an external mechanical loading the resulting strain for both is the same. The strain in the beam will be denoted by ε_b (which is the same for the sensor). The elastic modulus of the beam and sensor will be denoted by E_b and E_S respectively. The beam is symmetrical about the mid plane therefore, the strain will be ε_b and since total bending was assumed $\varepsilon_s=\varepsilon_b$. However, for the purpose of this project, the strain ε_b will induce equal value of strain on the sensor (ε_s). This strain (ε_s), will create a stress in the sensor which will manifest itself through the sensor voltage/charge output (dielectric

coefficient). The stresses applied are considered along the x-axis only. The bending stress on the compound beam is proportional to the bending moment which can be expressed by:

$$\sigma_{(x)} = \frac{M(x) \cdot H/2}{I} = -\frac{6P(L_b - x)}{BH^2} \tag{3.42}$$

Where:

$\sigma(x)$ is the bending stress on the beam surface (in N/m^2 or Pa)

$M(x)$ is the bending moment (in Nm) at a distance L_b-x from the point of load application $H/2$ is the distance from the neutral axis to the beam surface (in m)

I is the moment of area of beam cross-section (in m^4)

BH^2 is the section modulus of the beam (width and thickness in m^3).

The bending stress varies linearly from zero at the point of load application to a maximum at the clamped end (shown in figure 3.4). Also, it varies from zero to a maximum value (depending on the position of L_b-x) from the neutral axis to the surface of the beam. Thus in order to sense the beams deformation, the piezoelectric film sensor must be placed beyond the neutral axis of the beam (the closer to the surface the greater the response). The beam has a constant section modulus therefore the surface is in a uniaxial stress state and from Hook's Law this implies:

$$\varepsilon_b = \frac{\sigma(x)}{E} = -\frac{6P \cdot (L_b - x)}{E \cdot B \cdot H^2} \tag{3.43}$$

The corresponding strain and stress distribution are shown by the graph below.

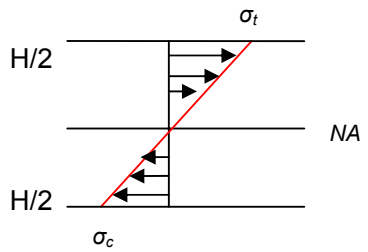

Fig 3.5 Strain and stress distribution in the beam due to external loading

3.2.3 The Bending Stiffness or Spring Constant of Composite Beam

From the expression for the maximum deflection of the bending beam shown in equation 3.41, we find the spring constant. The spring constant or stiffness is a measure of the rigidity or strength of the beam due to transverse loading.

$$w_{\max} = \frac{PL_b^3}{3EI}$$

$$but$$

$$P = kw$$

Therefore:

$$k_b = \frac{3EI}{L_b^3} \tag{3.45}$$

Considering the properties of the beam cross section, the above equation can be written as:

$$k_b = \frac{3E}{L_b^3}\frac{BH^3}{12} = \frac{EBH^3}{4L_b^3} \tag{3.46}$$

3.3 Bending Curvature to Voltage Relationship

As mentioned in chapter 2, piezoelectric materials generate a charge/voltage proportional to the rate of applied mechanical stress. In other words, when they experience a load, they respond producing a voltage/charge which varies with load magnitude. This property can be used to sense the behaviour of a structure under loading. On the other hand, the piezoelectric material also produces displacement/strain when a voltage/charge is applied thus enabling to also be used as an actuator to dynamically excite a structure.

In this project, piezoelectric sensors made of PVDF films are used to sense the behaviour of beams under loading conditions.

3.3.1 Static Sensor Equations

The deformation state of the composite beam (amount by which it bends under loading) can be monitored by the PVDF sensor embedded in it. A general voltage/charge-deformation relation formatted by Lee and Moon (1999) for a one dimensional model structure (beam or plate) can thus be used. Since strain is continuous in the beam-sensor interface as previously mentioned, a displacement applied across the PVDF material will generate a voltage which is the spatial integral

over the sensor. This can be expressed as:

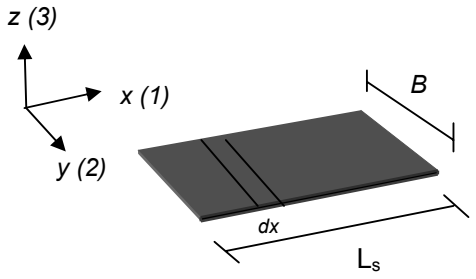

Fig 3.6 Rectangular Sensor strip

$$dV_s = \frac{e_{31}}{C}\varepsilon_s dA \tag{3.47}$$

Where:

e_{31} is the dielectric coefficient of the sensor material (which is the electromechanical coupling factor K_{31} divided by the stress constant or voltage coefficient g_{31}) in the longitudinal axis (1).

C is the sensor capacitance

ε_s is the strain in the sensor, $\varepsilon_s = \varepsilon_b = -z\frac{d^2w}{dx^2}$

dA_s is the differential area of the sensor which is the width *b* multiplied by *dx*

Therefore, from the above parameters and using the bending curvature relations the total voltage/charge produced by the sensor is given by:

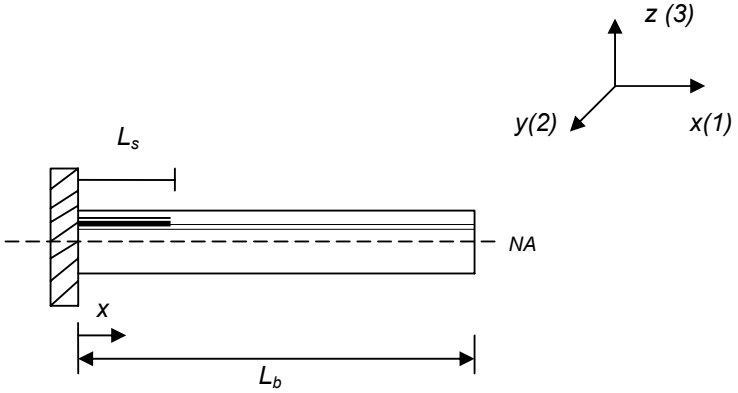

$$V_s = q_s(t) = -\iint_A b\frac{e_{31}}{C}\left(z\frac{d^2w}{dx^2}\right)dx = -zb\frac{e_{31}}{C}\int_{x_1}^{x_2}\left(\frac{d^2w}{dx^2}\right)dx = -zb\frac{e_{31}}{C}\Delta xk \tag{3.48}$$

Where:

k is the beam curvature which can be derived in terms of beam slope or displacement

$x_2 - x_1$ is the sensor position with respect to a reference point

The above equation shows that the sensor signal (as voltage output) is proportional to the local curvature of the beam or structure to be monitored.

3.3.2 Dynamic Sensor Equations

The charge generated by the sensor due to mechanical vibrations of the beam to which it is implanted will be detected when this charge is collected through the electrodes to an external measurement device. In other words, the charge collecting phenomenon performed by the electrode is equivalent to signal processing through the integration of spatial domain. The transverse deformation of the beam with the implanted PVDF sensor can then be decomposed in to the following modal summation:

$$w(x,t) = \sum_{i}^{\infty} A(t)X \tag{3.49}$$

Where:

A and *X* are the modal coordinate and mode shape, of mode i, from the beam equation of motion (described in the next chapter). *A* depends on the initial position (at *t*=0).

Substituting equation 3.49 in to deformation-charge relation described in equation 3.48 yields:

$$q_s(t) = \sum_{i}^{\infty} A(t)B \tag{3.50}$$

Where:

$$B = -ze_{31}\int_{x_1}^{x_2}\left[\frac{d^2 w_n(x)}{dx^2}\right]dx$$

Thus:

$$q_s(t) = -ze_{31}\int_{x_1}^{x_2}\left[\frac{d^2 w_n(x)}{dx^2}\right]dx \tag{3.51}$$

Where:

$$w_n(x) = \{[\cos(\lambda x) - \cosh(\lambda x)] + \sigma_n[\sin(\lambda x) - \sinh(\lambda x)]\}$$

The above equations allow for the measurement of charge/voltage signal of the sensor proportional to the mode shapes of the cantilever beam.

CHAPTER FOUR

ANALYSIS OF DAMAGE

4.1 Introduction

During the lifetime of a structure damage might occur due to an event or series of events. The presence of damage in a structure or system can compromise its safety under operating conditions. Thus, the need for inspection becomes an important task to undertake. The analysis of damage in structures and systems has produced an increased amount of study in the recent years.

In chapter three, the deformation of healthy beams with embedded sensors was discussed. The objective of the present chapter is to discuss the damage phenomenon giving a brief overview of different types, origin and damage models as well as the analysis of damage in cantilever beams.

4.2 Interpretation of Damage

Damage can be defined in different ways. One probably acceptable general definition is the degradation of a member or system when it undergoes a loading condition superior to what it is designed for or when it degrades due to usage. Scott et al (2003) defined damage as “changes introduced in to a system, either intentional or unintentional which affect the current or future performance of that system”. In many occasions, words such as defects and flaws are often used interchangeably to describe damage. Damage is normally associated with failure or yielding. A damaged structure or system may fail in different ways. Damage is considered to negatively affect the performance of a structure. It can cause loss of structure’s material properties or geometric configuration that may result in undesirable stresses, displacement or vibrations (Frederic, 1997).

From a wide perspective, damage could be anything from a void to a notch, to a crack, to a kink, which compromises the normal behaviour of a structure or system. Depending on the levels of exposure, certain types of damage may not show their effects for a long time. However, damage may be related to a number of surrounding factors which are associated with its initiation and propagation.

4.3 Types of Damage and its Origin

A wide variety of damage or defects can be found in a given engineering component. They can be classified in different types depending on their nature and material behaviour. Most common types of damage are related to fatigue, creep, corrosion, wear (typically found in metals), interlaminar/intralaminar delamination or debonding and fiber fracture (mostly found in composites). Crack damage is a type of damage that manifests with discontinuities at the scale of the structure. The discontinuity feature may be in the form of an interior or surface line crack which can take different shape, size and orientation. This type of damage is studied by fracture mechanics theory and has received a considerable amount of attention over the past years. The strength of the components or structures containing cracks is normally assessed by evaluating the stress concentration and intensity caused by the discontinuity feature.

Debonding or delamination is another type of damage typically found in layered/laminated materials and composites. The debonding normally happens at the interface of the laminate creating separation of the layers. The separation lowers both the compressive and tensile load carrying capacity of the structure. This type of damage has also received great amount of attention over the past years due to the increased usage of composite materials.

The damage described above, may result from material imperfections during the manufacturing process or generated during service and operation.

4.3.1 Material Imperfection

Regarding the first source mentioned, defects or damage can be found within the original material supply or can be introduced during the manufacturing process. On the microscale, typical material damage may include microvoid, microcrack nucleation and growth. The existence of distributed or concentrated voids, flaws and cracks of very small size can cause material degradation through strength and stiffness reduction (Hertzberg, 1996). For example, the handling of composite carbon and glass fine fibres requires special attention. The strength of the composite resides on the woven alignment and orientation (0/90, 45/45, 45/90 plies) which can be easily damaged if not properly handled.

4.3.2 Manufacturing Process

On the manufacturing side, damage may arise due to the use of improper methods and techniques. Many manufacturing methods like welding and composite forming may introduce defects in structures. In engineering, members in the form of cantilever beams are widely used. Cracks are likely to nucleate and grow in the tensile and compressive stress regions of the beams. Debonding of composite layers may occur due to improper use of bonding agents, resin mixture and curing time. The main consequence of these defects is to change the static and dynamic behaviour of these structures. Other examples include machining, grinding, and improper hardening laps (Hertzberg, 1996).

4.3.3 Operation

Most typical types of damage and failure occur under operation. Structural loading which causes bending, (tension and compression of members) twisting and torsion can in many occasions introduce defects or damage. For example, a rotating shaft in bending mode may crack around the entire periphery while one in unidirectional or reverse bending will have a crack surface generally confined to one or two locations (Bray &Stanley, 1989).

4.3.4 Environmental Conditions

Environmental conditions are also another aspect to consider as inflicting damage initiation and propagation in structures. For example, material degradation through corrosion damage can be observed in metallic structures. This normally happens due to exposure to climatic conditions such as rain, moisture and temperature variation.

4.4 Effects of Structural Damage

The effects of damage on a structure can be classified as linear or non linear. A linear damage situation is defined as the case where the structure remains in its linear elastic region after damage. The changes in the static and dynamic behaviour of the structure can be a result of changes in the geometric and or material properties of the structure due to moderate applied load that may alter parameters such as stiffness, mass and damping. However, its response can still be modelled using linear relations such as the Euler Bernoulli and Linear Elastic Fracture Mechanics (LEFM) theory.

A non linear damage case is defined as the case where the structure behaves in a non linear manner after damage has been introduced. In other words, the material does not obey linear elastic laws (Hooke's law). This type of damage normally leads to high discontinuities and non-uniform material behaviour. Large material deformations can induce non-linear behaviour contributing to damage. In such state, the material is no longer within the elastic limit. An example of non linear damage is the formation of intralayer delamination that grows along the length and width of a composite structure causing separation of the fibers (see figure 4.1). In such cases, due to the complexity of the problem, the material behaviour is normally modelled using Finite Element Method and complex analytical approaches.

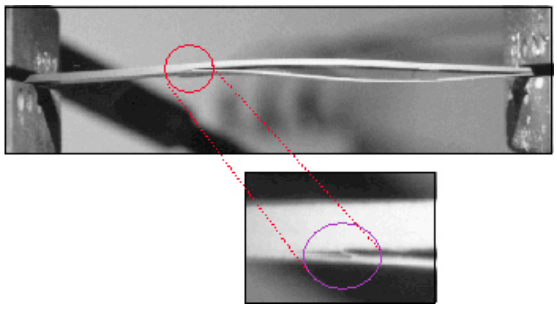

Fig 4.1: Interface crack delamination of composite beam (Stratton & Pelegri, 1999)

4.5 Formulation of Elastic Material Damage

The formulation of elastic material degradation which is normally used to describe the reduction of the stiffness property of materials starts from the basic notion of the effective area concept presented by Lazar Markovich Kachanov (1914-1993) which can be expressed as (Willian, 2002):

$$A_{eff} = A - A_d = [1 - d]A$$

(4.1)

Where:

$$d = \frac{A_d}{A} \text{ and } 0 \le d \le 1$$

represents the damage parameter.

Accordingly, the internal stresses in the material are transferred by the intact material. In other words, the presence of defects and stress concentration, reduce the effective load area as compared to the nominal area. This result in the effective stress concept through equilibrium considerations where:

$\sigma A = \sigma_{eff} A_{eff}$ which leads to $\sigma = [1 - d]\sigma_{eff}$

(4.2)

The strain equivalence concept:

$\varepsilon_{eff} = E\varepsilon_{eff}$ such that $\sigma = [1 - d]E\varepsilon$

(4.3)

The $[1 - d]$ factor reduces the elastic stiffness properties when d = 0 $\rightarrow$1 and is employed to represent the state of the damaged material or structure.

In order to characterise damage, additional features are incorporated beyond the basic format of the damage factor in order to account for different stiffness properties in both tension and compression to capture stiffness recovery due to different types of damage and loading conditions. According to Frederic (1997), in a damage detection model based on stiffness reduction, the physical mass of the structure may be conserved and damage can be represented as a change in the modulus of elasticity of the structure. An interpretation of this is that the damaged structure may preserve the same geometric properties of the original structure while the modulus of elasticity has been reduced. This can be considered as a valid interpretation to represent damage.

4.6 Damage Detection Model Approach

As mentioned before, the damage phenomenon has received an increased amount of attention among researchers in recent years. The ability to locate and assess damage in flexible structures is important for improving the performance and life span of these structures. Different methods have been proposed to model the damage state of a material structure or system. The aim of all models is to correctly or in some cases with approximations describe the behaviour of the structure in case. Aspects such as structural geometry and damage nature play an important role in defining the critical points of damage initiation and propagation.

There are two main approaches for damage analysis: The direct problem approach and the inverse problem approach. In the first approach, a mathematical model for the structure is constructed and used to develop an understanding of the structural behaviour and to establish correlations between specific member damage conditions and changes in the structural response (Cerri & Vestroni, 1999). These mathematical models are direct process models which follow from the causes of damage (nature, location and extent) to its effects (structural response). The second approach comprises of the identification of damage parameters based on experimental results. These results are then used to compare between a damage free model and a damaged model. Several papers have discussed the use of these approaches for modeling and damage detection in structures. In the damage detention models, analytical, experimental and numerical (FEM) or a combination of those have been used (Yin et al (1994), Peter & Donald (1998), Ishak et al (2001) Roseiro et al (2003), Saleh et al (2004), Isaksson & Hagglund (2005), Banan & Mehdi-pour (2007)). A popular model used for crack damage detection is the one in which the damage region is modelled by a rotational spring and the method normally calls for the search of the damage location and size. These have mostly been applied to cases of surface structural cracks of different size, shape and orientation.

In the present work, the inverse approach is used to detect internal flaws in composite beams equipped with embedded PVDF sensors. Static and dynamic measurements on healthy and composite cantilever beams with defects are conducted and used to validate a numerical FE model simulation. The defects which are intentionally made are assumed to occur between the layers of the composite beams and to extend through the entire width. The static measurements are used to determine the change in displacement of the free end and the apparent elastic property of the beams (due to the induced flaws at distinct positions along the beam's

length). The dynamic measurements are used to determine the natural frequencies of vibration of the cantilever beams.

4.7 Damage Analysis in Cantilever Beams

As previously mentioned, damage can be characterised by degradation of the elastic material property, as a result of a flaw or induced defect. This fact, normally tend to reduce the stiffness under loading. When a structure is subjected to a load, strain (deformation) and stresses are generated. If it happens that the defect is located either near or away from the maximum stress, the effect on the beam's static and dynamic behaviour will differ. The knowledge of the behaviour of the structure under load conditions can be used to create a damage detection scheme. In order to establish a damage scenario based on the inverse approach, a comparison of the behaviour between two different states of the structure: known as the undamaged or defect free state and the damage state is made.

4.7.1 Static Equations

For a damaged cantilever beam it is possible to approximate the bending curvature as:

$$\begin{aligned} w_D'' &= w'' + \Delta w'' \\ &= \frac{M}{EI} + \Delta\frac{M}{EI} \end{aligned} \tag{4.4}$$

Therefore the displacement equation can be expressed as:

$$\begin{aligned} w_D &= w_U + \Delta w \\ &= \frac{P(L-x)^3}{E_U I} + \Delta\left(\frac{P(L-x)^3}{E_U I}\right) \end{aligned} \tag{4.5}$$

Where:

w_U represents the displacement in the undamaged state

Δw_U represents the change in displacement due to inflicted damage

Since it is expected that the displacement of the free end of the beam is greater in the damaged state compared to the undamaged state. , the bending stiffness can be written as:

$$k_D = k_U + \Delta k_U$$
$$= \frac{3E_U I}{L_b^3} + \Delta\left(\frac{3E_U I}{L_b^3}\right) \quad (4.6)$$

4.7.2 Vibration Equations

The free bending vibration of a homogeneous uniform Euler-Bernoulli beam of constant rectangular cross section neglecting damping is given by the following differential equation (Ginsberg, 2001):

$$EI\frac{\partial^4 w}{\partial x^4} + \rho A\frac{\partial^2 w}{\partial t^2} = 0 \quad (4.7)$$

Where:

E is the elastic modulus of the beam material (GPa)

I is the second moment of area (m^4)

ρ and A represent the density of the material and cross sectional area of the beam respectively (in kg/m^3 and m^2)

Under vibrating conditions, the deflection at any point along the beam varies harmonically with time giving the above equation a solution of the form:

$$w(x,t) = X\left(A\cos wt + B\sin wt\right) \quad (4.8)$$

Where *X* is f(x) which defines the beam's shape of the normal mode of vibration. *A* depends on the initial position and *B* on the initial velocity. Both are determined from the spatial solution of the differential equation of motion which can be expressed as:

$$w(x,t) = w(x)e^{i\omega t} \quad (4.9)$$

Substituting in to the differential equation yields:

$$EI\frac{\partial^4 w}{\partial x^4} - \omega^2 \rho A w = 0 \quad (4.10)$$

Where:

ω is the frequency of motion (rad/s)

The general solution to the differential equation can be written as:

$$w(x) = C_1\sin(\lambda_i x) + C_2\cos(\lambda_i x) + C_3\sinh(\lambda_i x) + C_4\cosh(\lambda_i x) \quad (4.11)$$

C_1 to C_4 are arbitrary constants and λ_i is a frequency parameter (i =1, 2, 3...). Each

possible value of λ gives the mode shapes of the beam which depend on the boundary conditions imposed. For a cantilever beam these are:

$w(0,t)=0$ *no displacement at* $x=0$
$w'(0,t)=0$ *no rotation at* $x=0$
$w''(L,t)=0$ *no applied moment at* $x=L$
$w'''(L,t)=0$ *no applied shear at* $x=L$

The eigen solution can be expressed as:

$$\frac{\partial^4 w}{\partial x^4}-\lambda^4 w=0 \tag{4.12}$$

Where:

$$\lambda^4=\frac{\omega^2\rho A}{EI}$$

After solving for the constants the frequency characteristic equation can be written as:

$$\cos(\lambda_i)\cosh(\lambda_i)+1=0 \tag{4.13}$$

The solutions to λ_i which represent the eigen values can be expressed for the first three modes of vibration as:

$$\lambda_1=1.875 \qquad \lambda_2=4.694$$

$$\lambda_i=\left(\frac{2i-1}{2}\right)\pi \quad for\ i\geq 3$$

The equation for the solution to the natural frequencies in the undamaged case gives:

$$f_u=\frac{\lambda_i^2}{2\pi}\sqrt{\frac{EI}{\rho AL^4}} \qquad (\omega=2\pi f) \tag{4.14}$$

Where equation 3.13 is repeated here:

$$I=\frac{BH^3}{12}$$

The frequency values in the damaged condition can be expressed as:

$$f_D = f_U - \Delta f_U \tag{4.15}$$

Where:

f represents the frequency in the undamaged state

Δf represents the change in frequency due to damage

Thus:

$$f_D = \frac{\lambda_i^2}{2\pi}\sqrt{\frac{E_U I}{\rho A L^4}} - \Delta\left(\frac{\lambda_i^2}{2\pi}\sqrt{\frac{E_U I}{\rho A L^4}}\right) \tag{4.16}$$

Equations 4.6 and 4.16 allow us to estimate the free end displacement and natural frequency for the composite cantilever beams due to inflicted damage. However, these equations give a global estimate of the presence of damage due to a change in the elastic property. A more qualitative insight can be obtained by carrying an experimental investigation aimed at establishing the relationship between damage location and its effect on both static and dynamic conditions.

CHAPTER FIVE

EXPERIMENTAL AND NUMERICAL INVESTIGATION

5.1 Introduction

This chapter covers experimental tests which were conducted on flawed and defect free cantilever beams. The tests were aimed to determine the static and dynamic behaviour of the defect free and flawed beams equipped with PVDF sensors. The presence of defects changes the stiffness properties of the beam. This change, influences the static displacement (deformation) and natural frequencies (dynamic). Four specimens were manufactured in which three had internal flaws made intentionally during the manufacturing process. Static bending tests using masses applied at the tip end of the beams were carried out. The results of the free end displacements were used to determine the apparent elastic modulus and stiffness of the beams both in the undamaged and damaged case and possibly determine the defect location. Dynamic tests were also carried out to obtain natural frequencies using the embedded PVDF sensors and again the frequency variation indicating the flaw position. The tests results were used to validate a FE numerical simulation also discussed in this chapter.

5.2 Fabrication of Defect Free and Flawed Beams with Embedded Sensors

5.2.1 Making the Sensors from PVDF Film

There are different ways of making PVDF sensors from PVDF film as discussed in the literature. The sensors used for this investigation, were made from a 295mmx210mmx0.028mm S028NA0 PVDF film sheet (Supplied by Measurements specialties, USA). Rectangular shaped strips 25mmx20mm in size were cut from the film sheet using a roller cutter. Properties of the sensor are provided in table 5.1. Care was taken while handling the film to ensure it did not get damaged which would affect its high sensitivity. Appropriate gloves were used for the purpose. Copper foil conductive adhesive tape (supplied by RS components, SA) was attached to both sides of the film to capture the electric charge produced by the sensor, when activated.

Table 5.1: Sensor properties (Piezo Films, 2006)

Property	Units	Sensor
Mass Density (ρ)	Kg/m^3	1780
Elastic Modulus (E)	GPa	2.5
Dielectric Constant (e_{31})	C/m^2	0.046
Permittivity (ε)	10^{-12} F/m	106

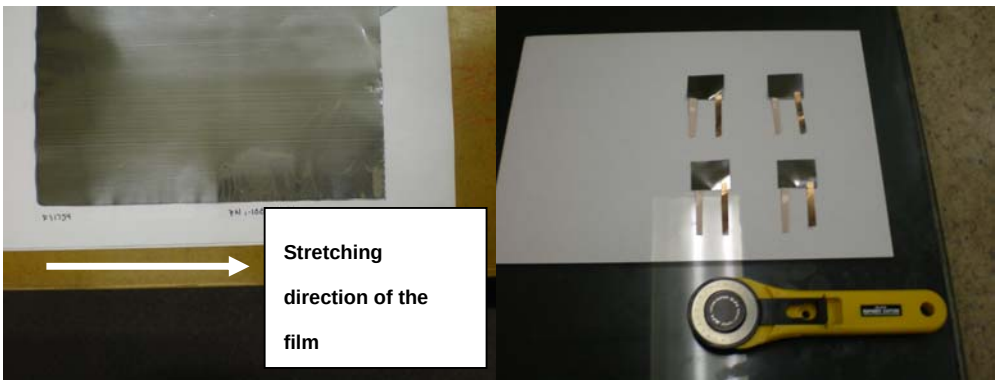

Fig 5.1: Sensor from PVDF film

5.2.2 Material Preparation and Fabrication Method

The defect free and flawed beams were manufactured from a 500mmx500mmx1mm clear Poly Methyl Methacrylate (PMMA) extruded sheet (also known as acrylic glass or Perspex). The sheet was properly clamped and cut using a sharp stable nife (Irwin) in to rectangular specimens with a size of 145.5mmx 27.75mmx1mm. The fabricated beam specimens consisted of five layers of acrylic glass and a strip of embedded PVDF film sensor. The layers were glued together using chloroform. Chloroform is a low viscosity volatile liquid which provided a clear and strong bond. The sensors were embedded between the first and second layer from the top. They were all aligned in the same position near the fixed end of the specimens. Flaws were introduced between the second and third layer by isolating a section along the beam length using transparent adhesive tape. The adhesive tape prevented the chloroform to contact the isolated area thus creating a separation between the second and third layers on that section. The chloroform was poured along the entire area of the beams using a syringe. The beams were stacked one upon the other. The flaws were made intentionally to simulate manufacturing imperfections which would compromise the elastic properties (stiffness) of the beams. In total four specimens

were fabricated. One was made defect free and the rest had flaws with a length of 35mm at distances of 47.5mm, 82.5mm and 117.5mm respectively from one end of the beam to the centre of flaw area. The process was carried at room temperature. The specimens were left for 24 hours to ensure proper bonding and all have a thickness of H= 5.80mm.

PMMA rectangular sheet

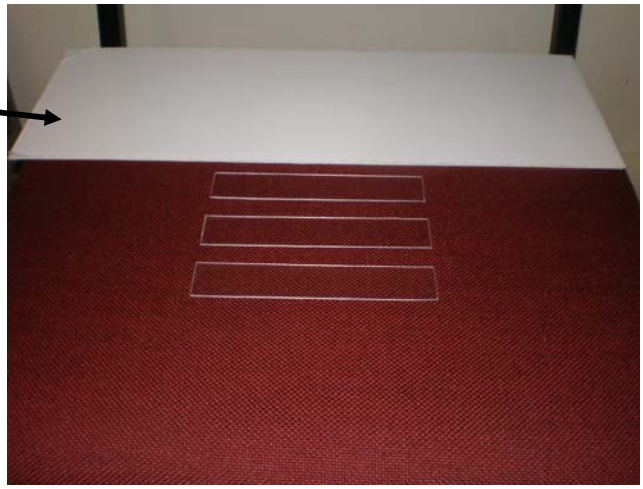

Fig 5.2: Specimens Material (PMMA)

Fig 5.3: Components used for specimen fabrication

Earthed wires were soldered on the conductive copper adhesive attached to the sensors by using an adjustable temperature lead solder. An advantage of making the sensors with copper conductive adhesive is that it prevents high soldering temperatures to get in direct contact with film which could cause depoling of the piezoelectric material and degradation of the silver coating (electrodes). The soldering temperature was maintained at 350˚C.

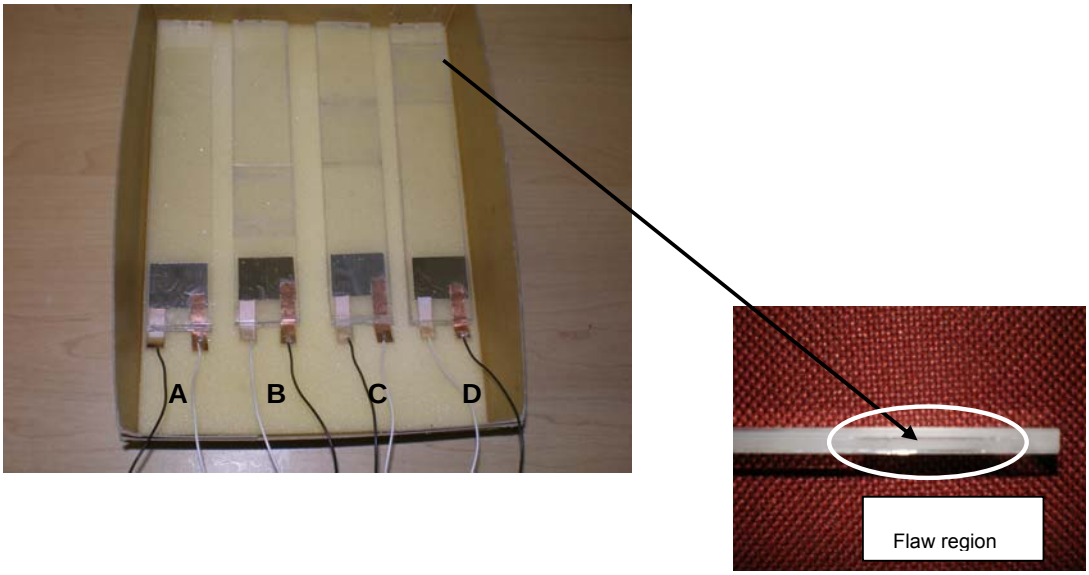

Fig 5.4: Fabricated defect free and flawed beams with embedded sensors

From left, A: Defect free specimen, B: Specimen with flaw at a distance 47.5mm, C: Specimen with a flaw at a distance of 82.5mm, D: Specimen with flaw at a distance of 117.5mm

5.3 Experimental Procedure

5.3.1 Static Displacement Measurements

Free end static displacement measurements were performed to determine the apparent modulus of elasticity of the defect free and flawed beams. The beams were clamped at one end to a cantilever test fixture (near the sensor location) while the other end was left free. Measurements of static displacement of the free end of beams were obtained with the help of a digital dial gauge with an accuracy of 0.001mm, full spring compression of 14.25mm. The dial gauge tip was brought in to contact with the free end tip of the beam. A mark at the tip free end of all beams was made exactly at the same distance to serve as the tip contact point. Masses with size of 50g, 100g, 150g, 200g, 250g and 300g respectively were applied while attempting to measure the displacement. The measurements were repeated several times to ensure consistency in results. The experimental setup for measuring the displacement due to applied load at the free end of the beams is shown in figure 5.5.

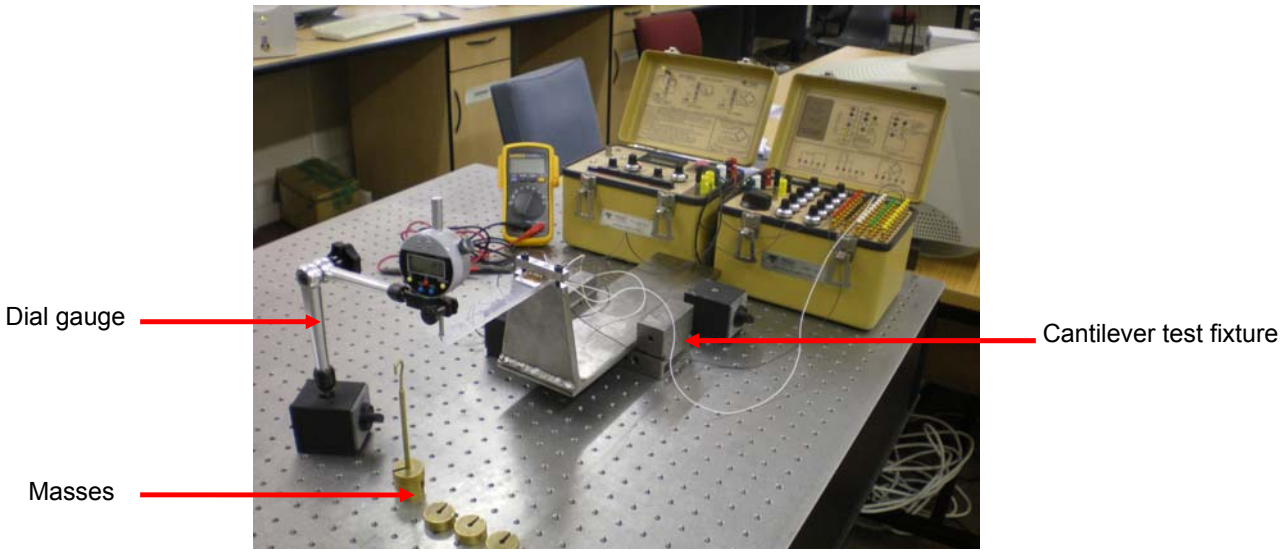

Fig 5.5: Experimental set-up for displacement measurements

5.3.2 Frequency Measurements

The main purpose of this experiment was to use the embedded PVDF film as the sensing device to detect the changes in natural frequency due to the presence of flaws. The components in the experimental setup for the natural frequency measurements consisted of a function generator (Arbitrary Function Generator Model: GW Instek GFG- 8216A310), digital real time oscilloscope (two-channel Model: TPS 2012 Sony Tektronix 100MHz-1Gs/s), connecting probe (voltage probe Model: P2220 Sony Tektronix 200MHz/6MHz-16pF/95pF, 10x/1x resolution), Mosfet audio amplifier (Star sound Model: SSA-1060, 400W), DC power supply (Ultra power prolux AC:100-240V-DC:12V, 10 amps), and a loudspeaker (7.5W-16ohms EAS4T101S). The function generator produces a 0.5V volts (peak to peak) sine signal to the loudspeaker. The audio amplifier is powered by the 12V DC power supply and receives the input from the function generator channel to the output (loudspeaker). The acoustic field excited by the loudspeaker vibrates the beam. In steady state, the beam vibrates at the frequency of the driving force. When the driving force is at a normal mode frequency, the energy transmission is efficient, so the beam has maximum surface displacement and vibrates at its resonant frequency. A real time oscilloscope is connected to the beam sensor terminals via the probe and displays the output response of the sensor to the beam's vibration. Two measurement options were used with the oscilloscope:

Time domain measurements – the time domain option allows for measurement of displacement (as amplitude, normally in volts) of the periodic wave form generated

due to vibration of the specimen.

Frequency domain – in frequency domain, the Fast Fourier Transform (FFT) mathematic program build in the oscilloscope is used to obtain the resonance response of the beams from the time domain measurements. The speaker is positioned to cover the entire beam length with central woofer (where maximum displacement of the speaker occur) located 100mm from the fixed end of the beams. Input frequencies ranging from 1 to 500Hz were selected on the function generator while attempting to measure the natural (resonance) frequencies of the beams using the embedded sensors. The experimental setup for measuring the frequency of the beams is shown in figure 5.6.

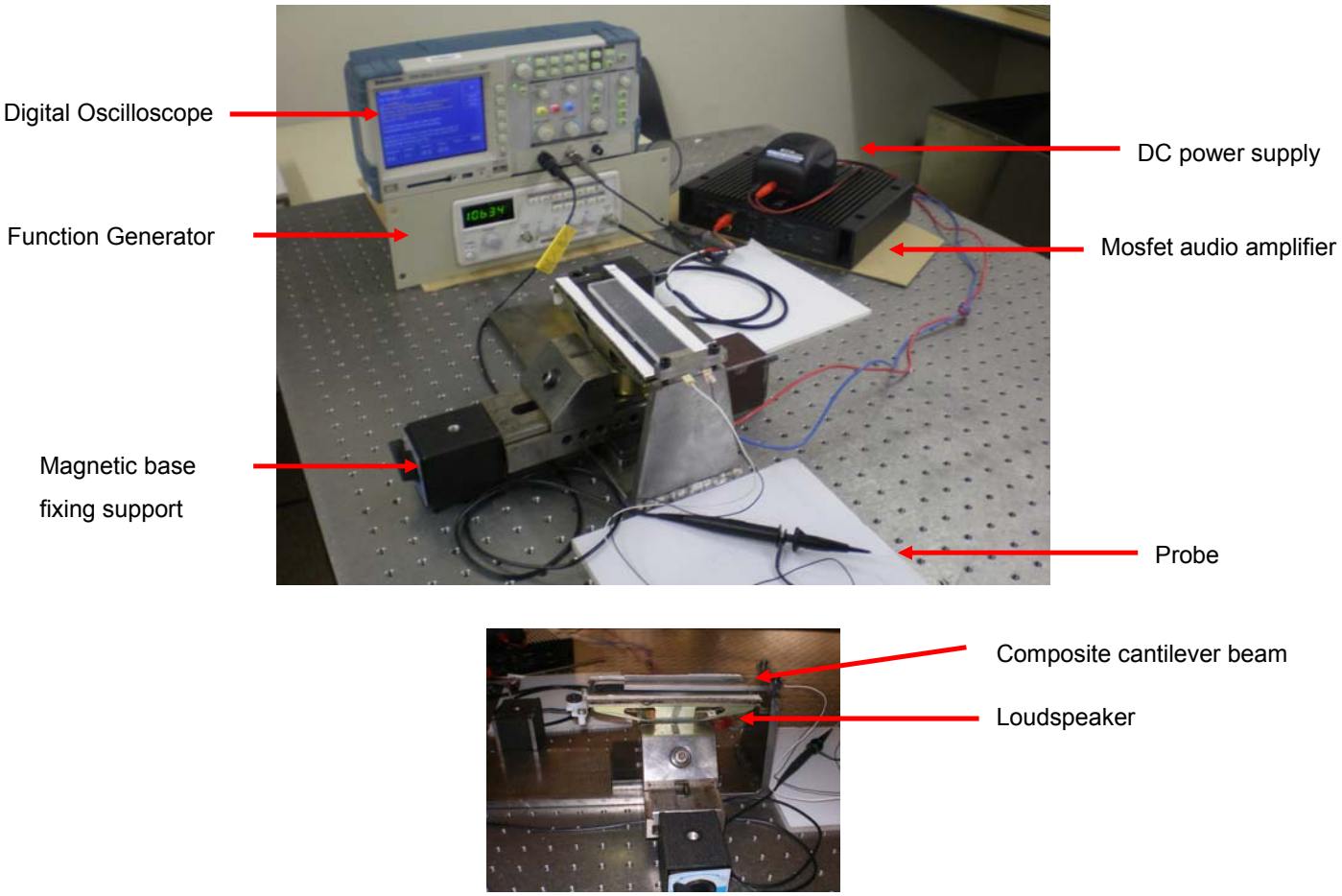

Fig 5.6: Set up for dynamic measurements

The frequency measurements were repeated several times to ensure consistent measured values were obtained.

5.3.3 Results and Discussion for Static Displacement Measurements

Flaws closer to the fixed end of the beams result in higher free end displacement which indicates reduced apparent elastic modulus and stiffness compared to flaws closer to the free end. The apparent elastic modulus is higher for the defect free beam as expected and decreases as the flaw moves towards the fixed end of the beam. The obvious reason is that near the fixed end deformation varnishes and higher stresses are captured. On the other hand, near the free end of the beam stresses are very small and maximum deflection occurs. This demonstrates that the stress discontinuity introduced by the defect influences the stiffness as the elastic modulus is related to the strain and stress. Displacements for the different applied loads indicate a linear relationship between them.

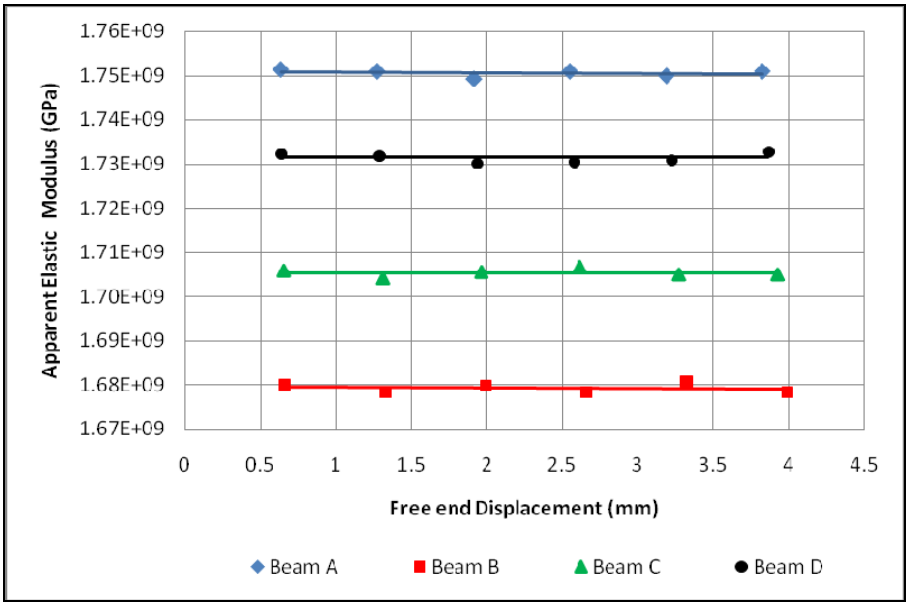

5.7 Fig: Apparent elastic modulus for defect free and flawed beams

5.3.4 Results and Discussion for Frequency Measurements

As with the static case, the dynamic case follows a similar pattern. The variation in natural frequency is dependent on flaw position. As the flaw position moves away from the fixed end so does the natural frequency, approaching the defect free beam's natural frequency. The reduction in frequency from the defect free beam to the first flaw position is in the order of 2.5% decreasing towards the fixed end.

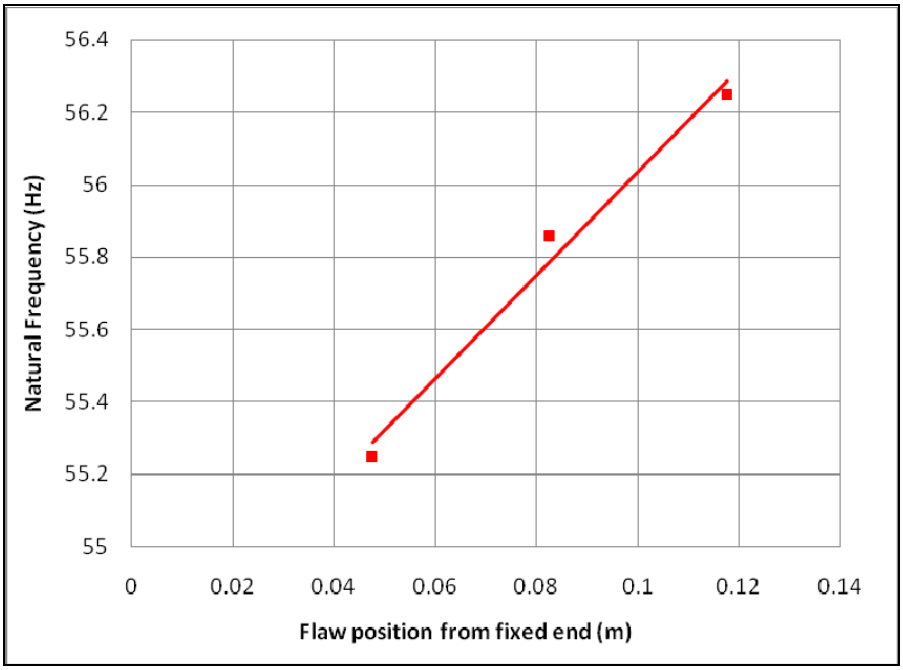

Fig 5.8: Frequency of flawed beams as a function of position

In the above tests, four composite cantilever beams with embedded PVDF sensors in which three had localized flaws have been experimentally tested. The results obtained demonstrate that the flaw position is an important parameter in behaviour of the cantilever beam under load.

5.4 Numerical FE Simulation for Predicting the Beam's Behaviour

In order to predict the effect of damage size and location on the behaviour of a cantilever beam a Finite Element (FE) simulation using commercial software was conducted. FE is a computer aided mathematical technique to approximate numerically the behaviour of a structure. The method essentially consists in dividing a model of a structure in to small discrete pieces called elements that are connected together at a finite number of points called nodes. With structure divided in to elements, it is possible to analyse using the procedure similar to that in beam theory.
In order to have a simple representative model in terms of the analysis procedure and computational time, the damaged model (beam) is represented by a reduction in *E* at distinct locations. Two type of analysis were performed: Static and vibrational. The static analysis was performed in order to obtain the relationship between damage size and position on the deformation of the beam's free end. The vibrational analysis was performed to generate the frequencies and establish the relationship between damage location and natural frequency.

5.4.1 Software Description

The software used for the numerical simulation was ANSYS V11, a multi-purpose finite element software with modeling and simulation capabilities. It is used across many disciplines in the science and engineering field for a wide range of numerical analysis such as linear and nonlinear response of structures and systems, buckling and fatigue, modal and harmonic response, heat transfer, electromagnetic, magnetostatic and computational fluid dynamics (CFD). It is powerful and user friendly with interface capabilities with other design and simulation software. The program contains two main features: the pre-processing and post processing. The pre-processing is the input part in which the user defines the geometry of the structure been analysed as well as all other analysis data required (real constant, material properties, loads, etc.). The post-processing allows to review the results of the analysis.

5.4.2 Finite Element Model and Analysis Procedure

The model of a beam with a damaged segment can be represented by a beam with a zone of reduced elastic modulus due to flaw E_D compared to the rest of the beam E_U. The parameters adopted to define the damage are the position X_i from the fixed end of the beam to the centre of the damage zone, the length L_D of the damage also with respect to the fixed end, and the percentage of stiffness loss β due to change in E. These can be represented by:

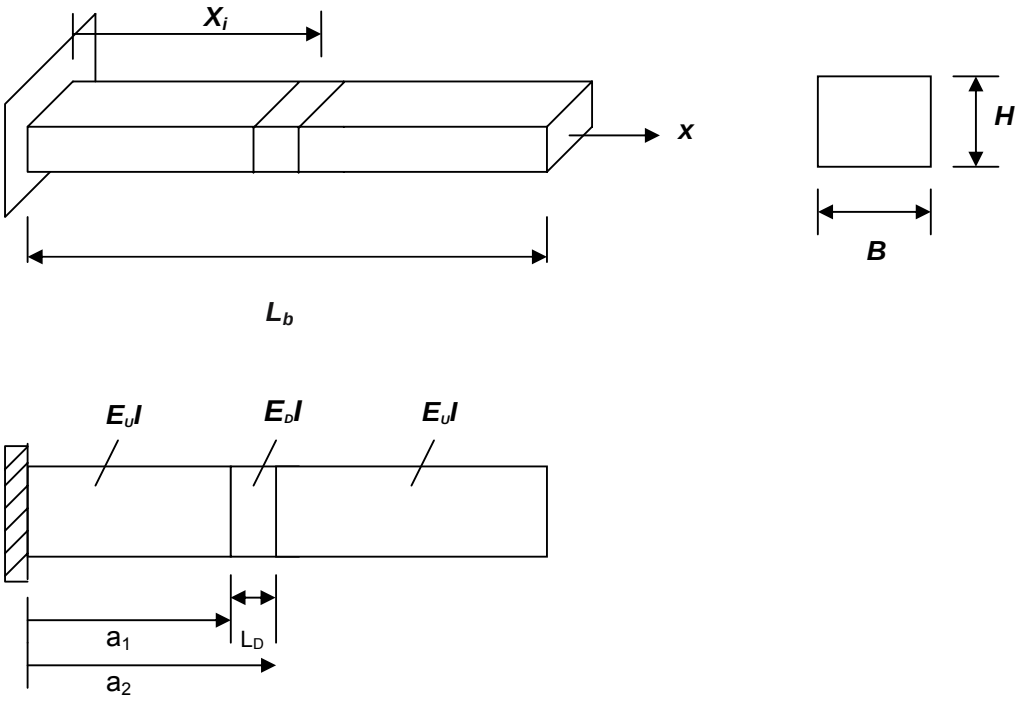

Fig 5.9: Damage model of the beam

$$L_D = a_2 - a_1$$

$$\beta = \frac{E_U I - E_D I}{E_U I}$$

The following assumptions are made regarding the damage in the beam:

I. The damage is represented with a small change in elastic modulus that affects the stiffness of the beam

II. The geometrical configuration of the beam remains unchanged (cross section)

III. In the damaged state, the beam is considered to remain in the elastic region

IV. Damage occurs within the domain of the system and the boundary conditions for static and dynamic case remain unchanged compared to the undamaged case

The defect free and flawed beam models were drawn using Solidworks V2007 and imported to ANSYS. Each beam used to represent the defect model was

constructed by assembling three rectangular sections which were mated and connected by contact parameter in ANSYS. ANSYS has different options for contact and formulation approach such as bonded, separation, rough and frictional contact with pure penalty, normal Lagrange and augmented Lagrange.

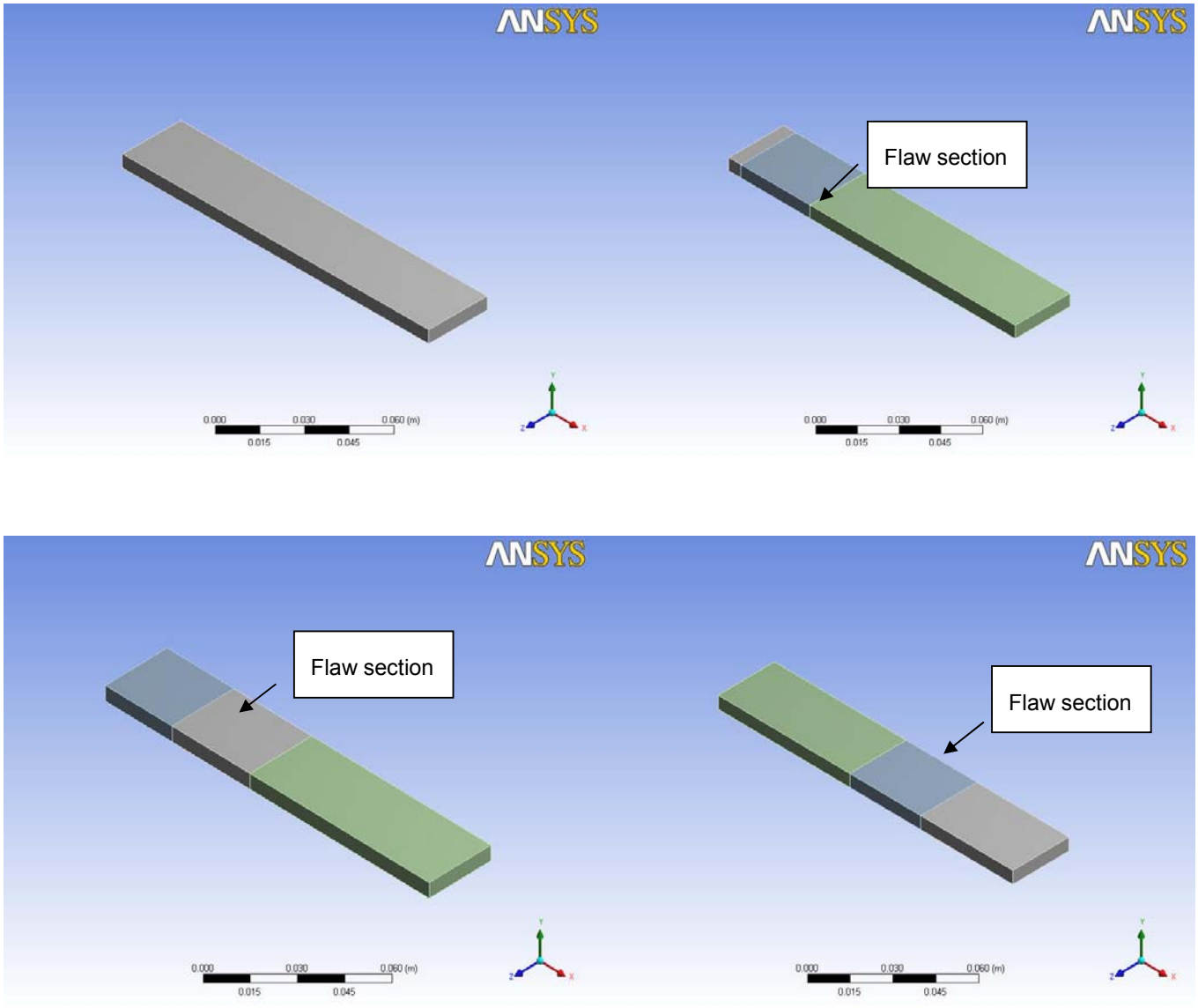

Figure 5.10: Defect free and flaw beam models in ANSYS

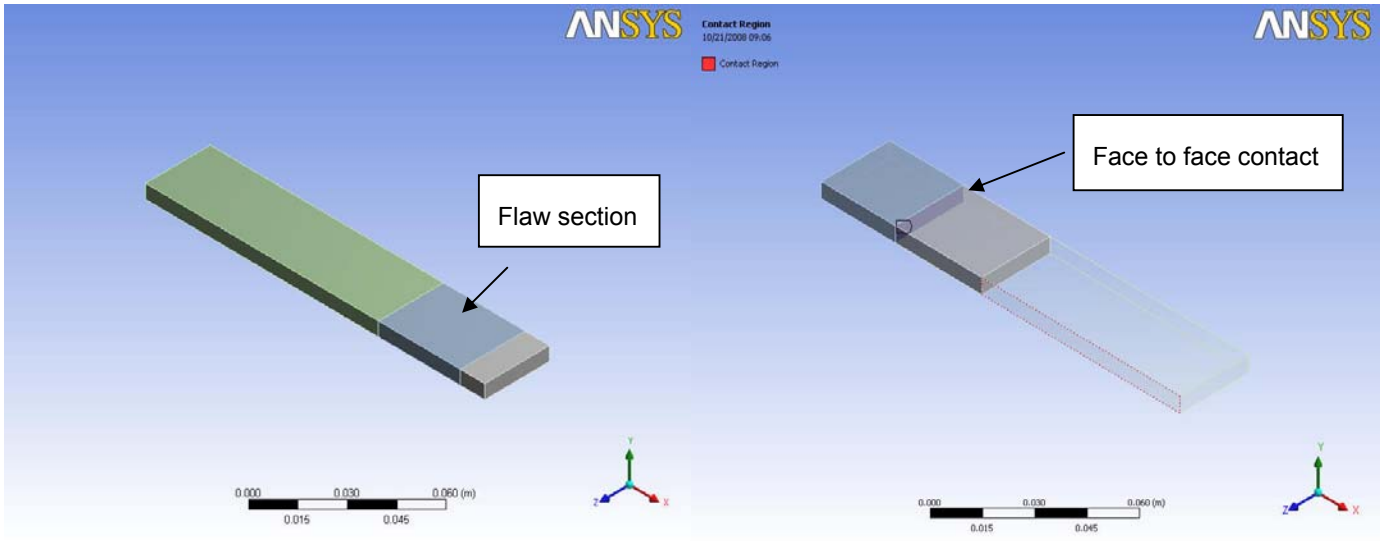

Figure 5.11: Flawed beam model and contact parameter

The contact parameter, describes how the parts (rectangular beams) are connected and move relative to one another. In this case, the bonded type contact with pure penalty formulation method was used. The bonded contact prevents sliding or separation between the faces and edges of the parts joined together. Pure penalty is a formulation method which satisfies contact conditions by preventing penetration between contact parts so that the structure assembly behaves as a one solid unit. Five beam models were built. Solid 186 element type was used for the analysis. This is a higher order 3 dimensional 20-node solid element that exhibits quadratic displacement behaviour. The element is defined by 20 nodes having three degrees of freedom per node: translations in the nodal x, y, and z directions. New material properties for the beam models were created and set in the material properties database (see table 5.2).

Table 5.2: Material properties of composite beam

Property	**Units**	**Beam**
Density (ρ)	Kg/m^3	1238.35
Apparent Elastic Modulus (E)	GPa	1.75

The beams were meshed with 25 elements per division (which correspond to the ratio of length over thickness). The mesh describes the division of the structure in to elements that are joined together by nodes to represent the model. Because the beams with defects consisted of assembled models the mesh distribution is higher compared to the defect free.

More elements and nodes are required to mesh the models to prevent high stress generation.

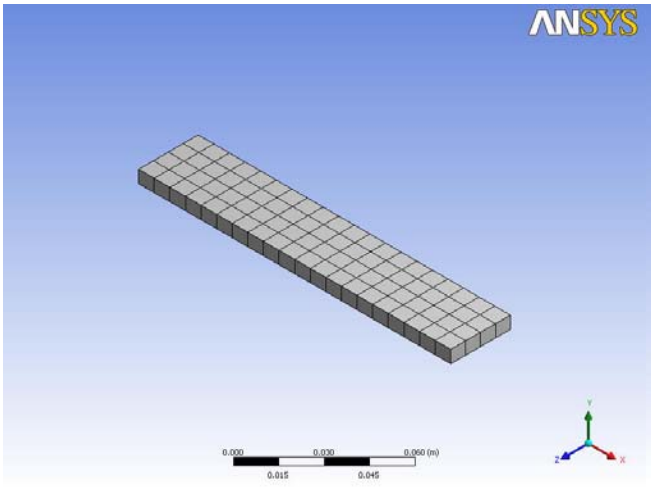

Elements: 80 Nodes: 683

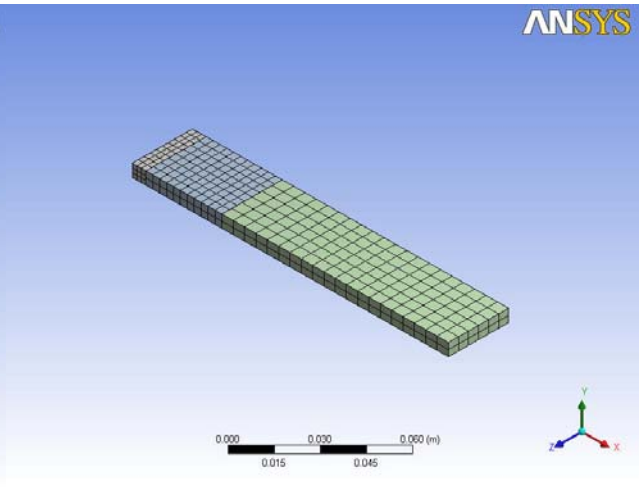

Elements: 532 Nodes: 3413

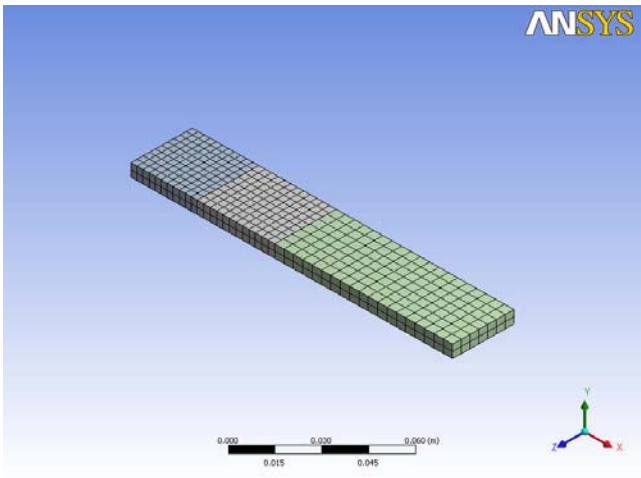

Elements: 702 Nodes: 4420

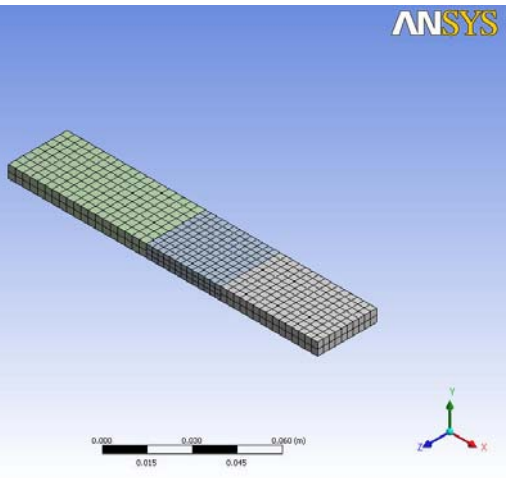

Elements: 994 Nodes: 5958

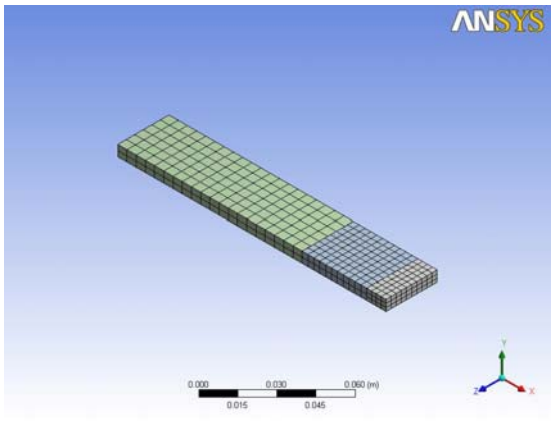

Elements: 558 Nodes: 3548

Fig 5.12: FE Mesh of Defect free and flawed beams

In order to simulate the beam models as a cantilever (with one end fixed and the other free), fixed constraint was applied to the left end of the beams to prevent any motion. Rotations and translations in the 3 dimensions: x, y and z were set to zero.

5.4.3 Static and Dynamic FE Equations

The equation for the static analysis of the finite element model is:

$$[K]\{u\} = \{F_{app}\} \tag{5.1}$$

Where:

[K] = Total stiffness matrix (sum of element stiffness matrices)

{u} = nodal displacement vector

$\{F_{app}\}$ = Applied nodal force load vector

The dynamic equilibrium equation of the finite element model neglecting damping can be expressed as:

$$\left([K] - \omega^2[M]\right)\{\varphi\} = \{0\} \tag{5.2}$$

Where:

[*K*], [*M*], ω and {Φ} indicate the stiffness matrix of the structure, global mass and eigenvector (related to the mode shape) respectively.

5.5 Case Study: Effect of Flaw Position on the Response of the Cantilever Beams

In order to numerically investigate the effect of flaw position on the static response of the cantilever beams, each rectangular section representing the flaw area has a length of a_2-a_1= 35mm. The sections are located at a distance *Xi* = 23.75mm, 47.5mm, 82.5mm and 117.5mm respectively from the fixed end of the beams (at the left hand side of the models). The defect free and flawed beams have a total length L_b = 145.5mm, width *B*=27.75mm and height *H*=5.8mm. The elastic modulus at the flaw section was reduced to E_D= 1.64, 1.50, 1.30 and 1.15 GPa respectively. Loads with value of 0.4905N, 9.81N, 1.4715N, 1.962N, 2.4525N and 2.943N respectively were applied to the free edge of the beams. The results for E_D=1.50 which corresponds to β=0.14 are presented here.

5.5.1 Simulation Results under Static Loading

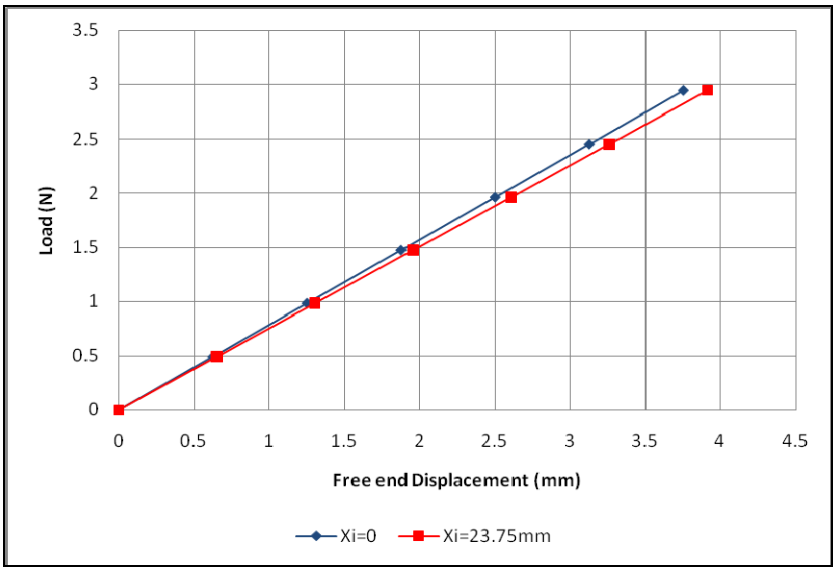

Fig 5.13: Load Vs Free end Displacement for flawed beam at: X_i=0 and 23.75mm

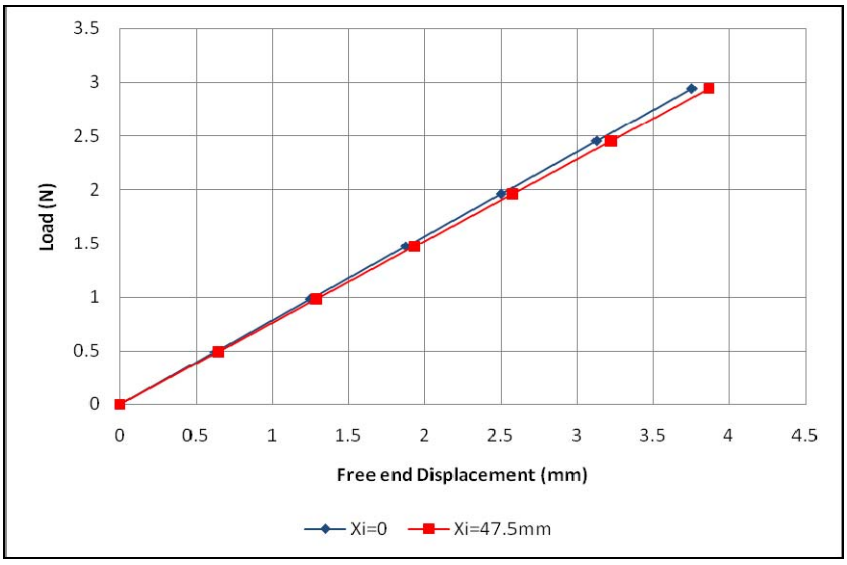

Fig 5.14: Load Vs Free end Displacement for flawed beam at: X_i=0 and 47.5mm

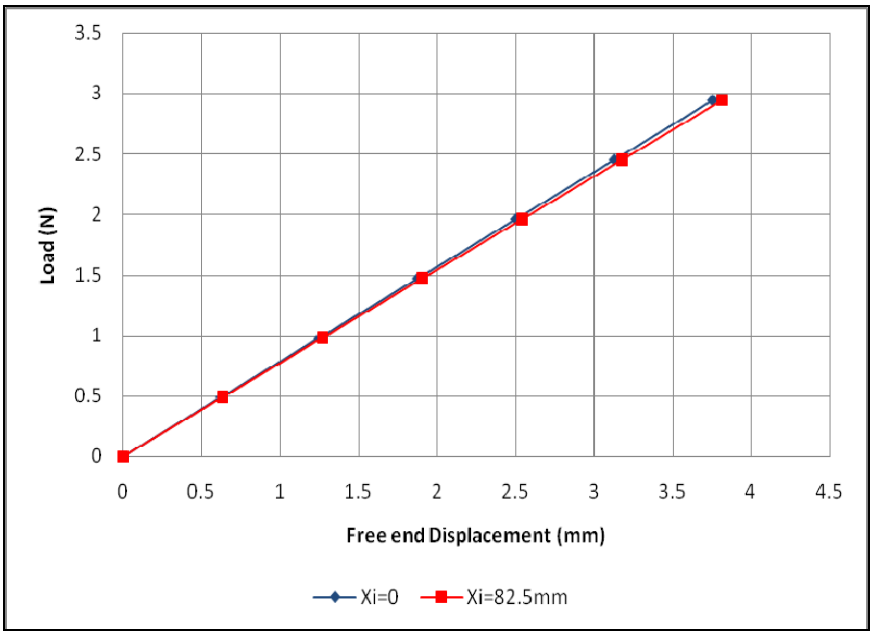

Fig 5.15: Load Vs Free end Displacement for flawed beam at: X_i=0 and 82.5mm

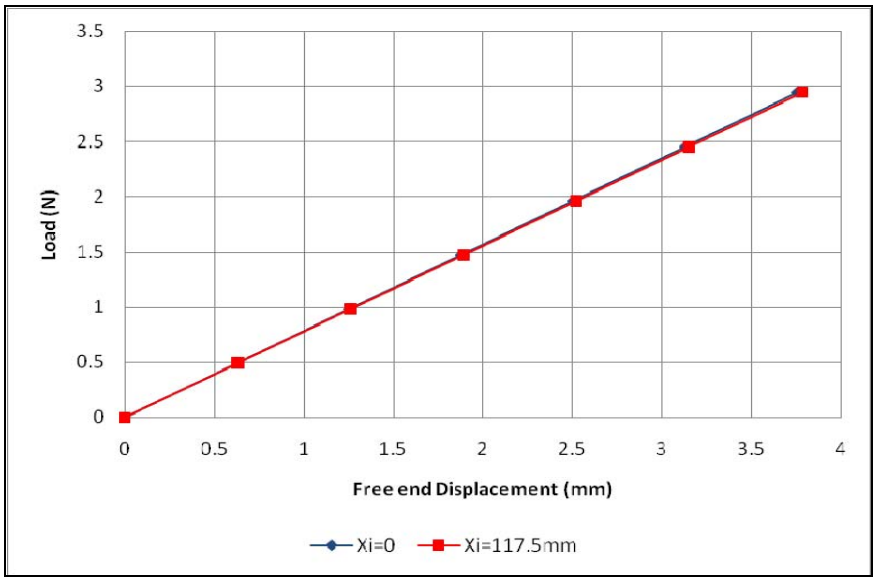

Fig 5.16: Load Vs Free end Displacement for flawed beam at: X_i=0 and 117.5mm

In the above figures, the beams with defect at different locations were plotted against the defect free beam. As the flaw position gets further away from the fixed end, the displacement decreases approaching the displacement values for the defect free beam. In other words, the closer to the fixed end the greater is the displacement. Also, for each specific location, a reduction in elastic modulus causes an increase in displacement but again more noticeable near the fixed end. This suggests that flaws

located near the fixed end of the beam are more critical causing a greater reduction in the load carrying capacity of the beams which agrees with the experimental obtained results.

The effect of flaw position on the dynamic performance of the cantilever beams was also considered. The same beam models for the static analysis were used. The first natural frequency for the beams with flaws at the above specified positions were obtained. Block Lanczos mode extraction method was used to generate the frequency of the beams. In the modal analysis damping effects due to energy dissipation are neglected.

5.5.2 Simulation Results under Dynamic Loading

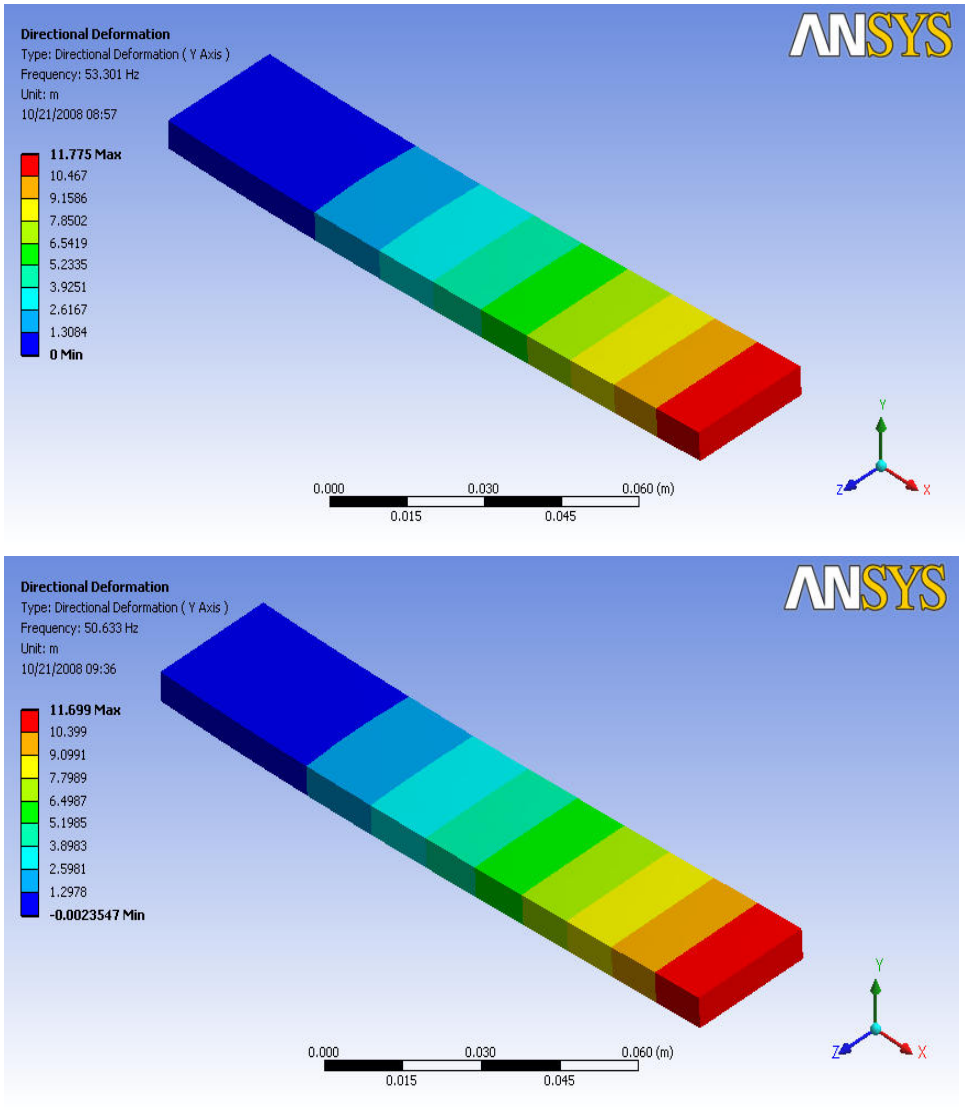

Figure 5.17: Defect free and flawed beam at X_i= 0 and 23.75mm under dynamic loading

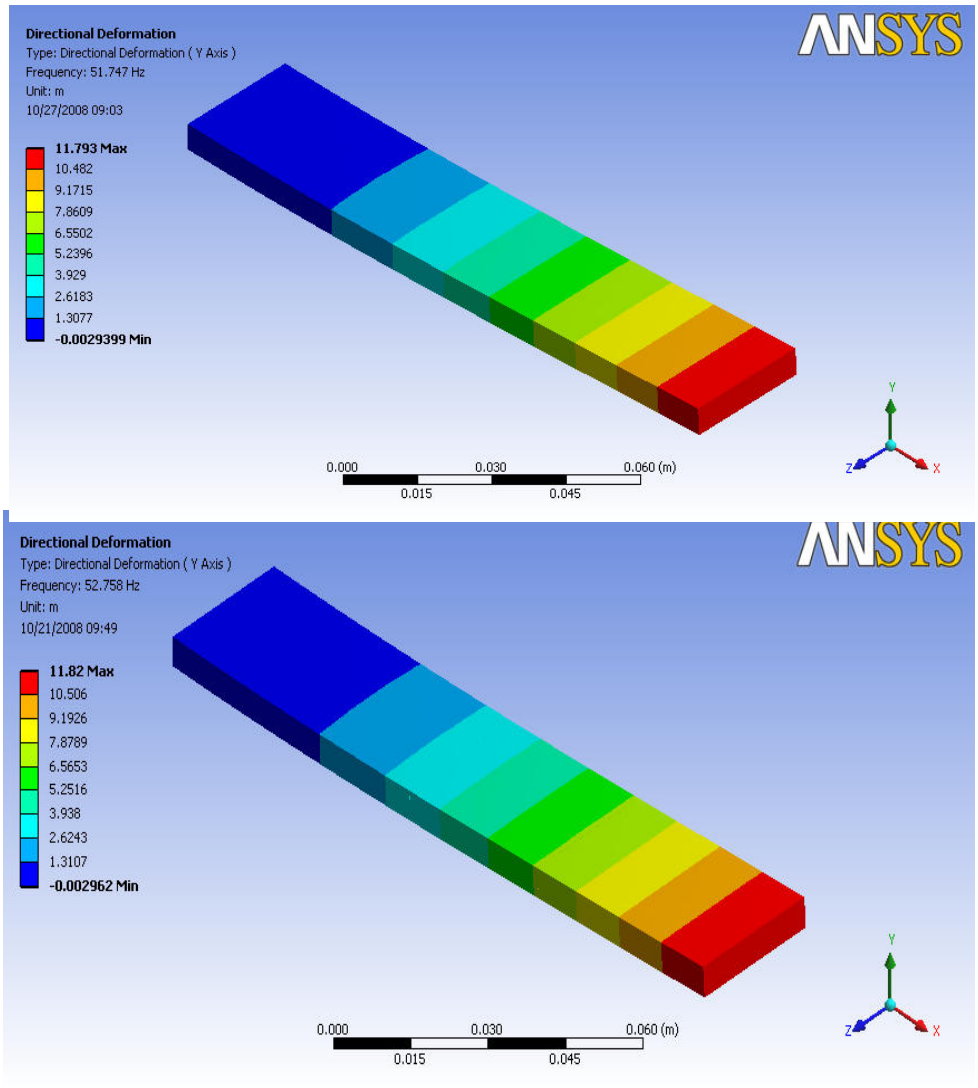

Figure 5.18: Flawed beams at X_i= 47.5mm and X_i= 82.5mm under dynamic loading

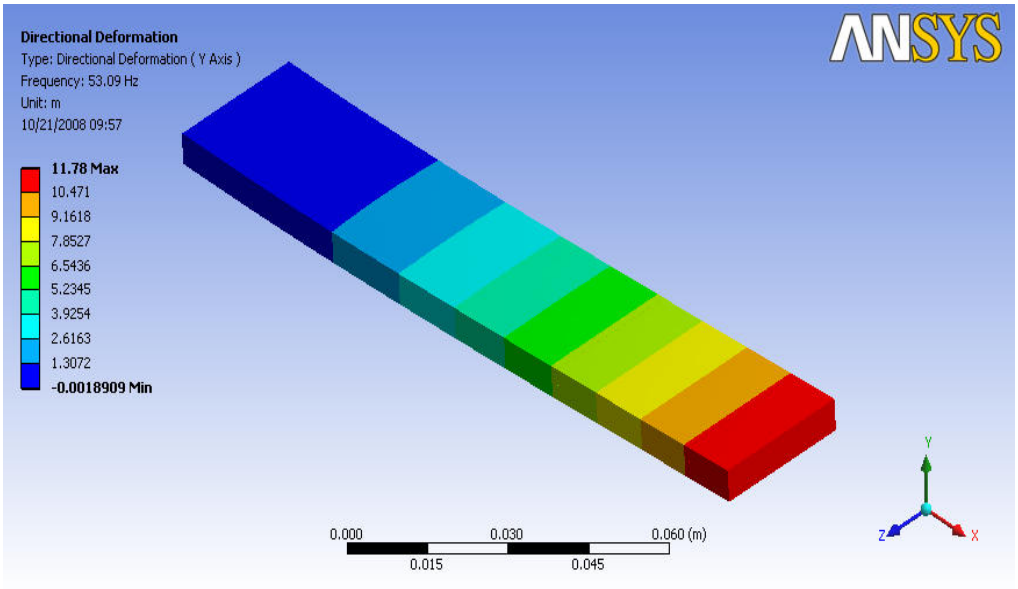

Figure 5.19: Flawed beams at X_i=117.5mm under dynamic loading

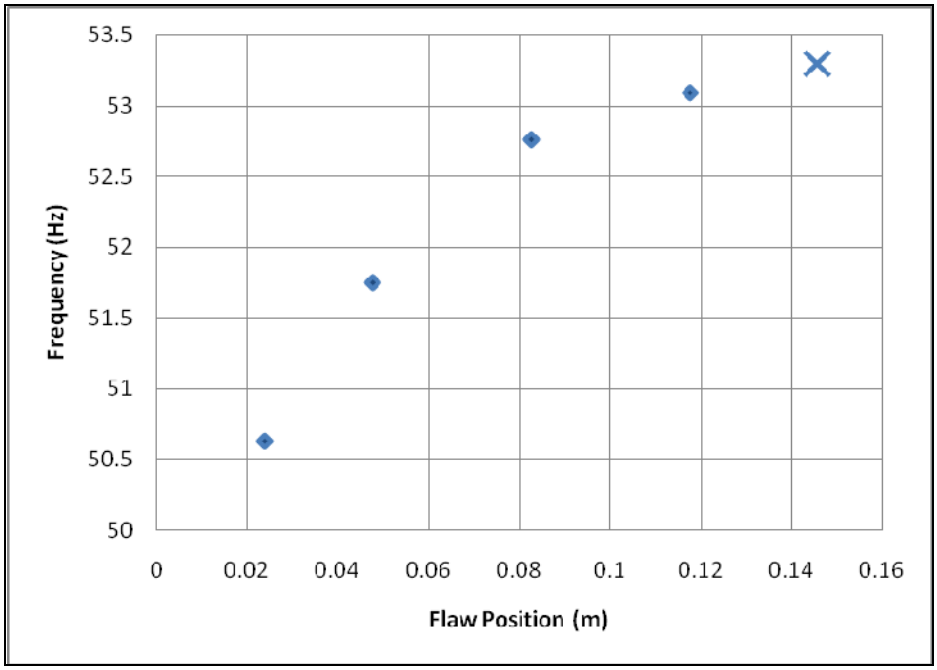

Figure 5.20: First mode frequency Vs flaw position

Figure 5.20 depicts the effect of flaw position on the frequency of the beams. As the flaw location changes so thus the frequency of the beams. Again the same behaviour as with static case is observed. The closer to the fixed end the lower the frequency

and vice-versa. Also, moving the flaw near the free end renders a frequency value close to the defect free case. However, the graph does not follow a rigorous linear path, there is a tendency to curve as the flaw position approaches the free end. Therefore, the last point on the graph was obtained by extrapolation assuming a frequency value equal to the undamaged beam at the free end.

The deviation of frequency values from the defect free to the first flaw position is in the order of 5% and decreases as the flaw position increases from the fixed end. From the above graph, it is possible to deduce or predict the flaw location based on the frequency value within the boundaries of: $L_b > x > 0$.

5.6 Comparison between FE and Experimental Results

Table 5.3: FE and Experimental Results for Defect free and flawed beams under dynamic conditions

FEM Values		% difference	Experimental Values	
Flaw Position X_l (m)	Natural Frequency mode 1 f (Hz)		Flaw Position X_l (m)	Natural Frequency mode 1 f (Hz)
0	53.3	5.96	0	56.68
0.0475	51.75	6.33	0.0475	55.25
0.0825	52.76	5.55	0.0825	55.86
0.1175	53.09	5.62	0.1175	56.25

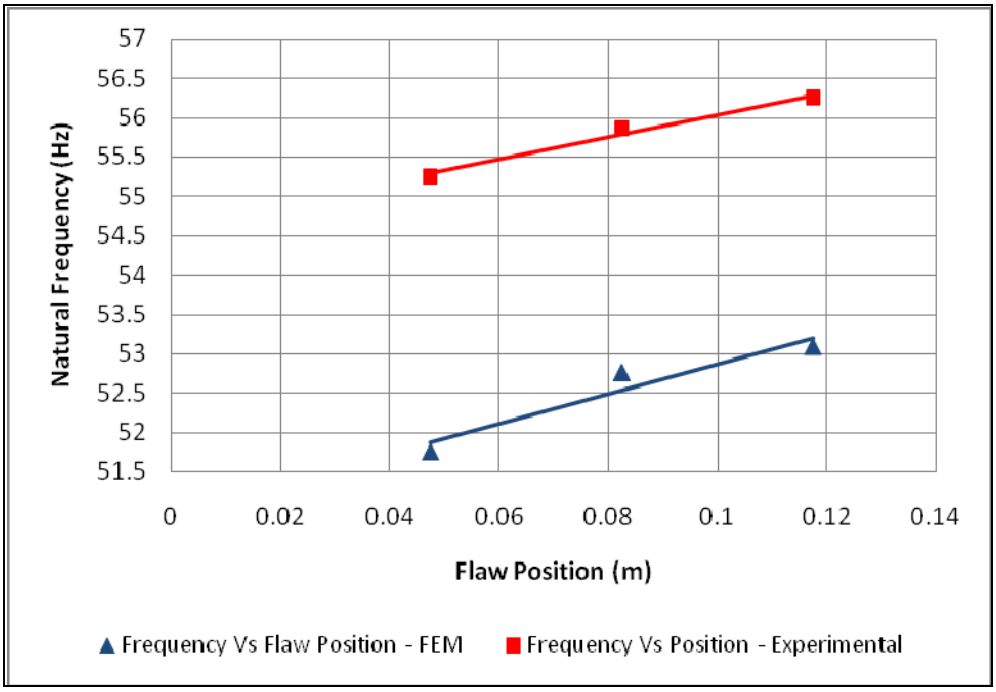

Fig 5.21: Frequency Vs Flaw Position –Experimental and FE Results

The experimental results obtained are in good agreement with numerical ones. The slight difference in results can be justified by the following reasons:

- Modeling of the thin PVDF sensor which was not included in the numerical simulation
- Accuracy in measuring the experimental beam models
- Properties of the bonding layer which have been neglected

CHAPTER SIX

CONCLUSIONS AND RECOMMENDATIONS

6.1 Introduction

The detection of damage in materials and structures is part of Structural Health Monitoring (SHM) systems which has as primary objective to monitor and assess the status of the integrity of a structure based on reliable methods. The focus of this research was to develop a good understanding of the theoretical and practical framework of PVDF piezoelectric materials and couple them to a particular case as an example where they could be used for damage detection.

6.2 Research Outcomes

The objectives set for this work have been met. Deformation and damage detection in composite beams equipped with PVDF sensors have been conducted experimentally and the results were used to validate an FE model. The proposed method based on numerical and experimental data to predict the effect of damaged parameters (elastic modulus and location) on the beam's response to quasi-static and dynamic loading, has shown that for the type of damage considered, its relative location along the beam length affects the static and dynamic conditions. This has been numerically simulated for various reduction in elastic modulus and locations. The loss of local stiffness is related to the damage location along the structure and areas of maximum stress. For the static case, a reduction in elastic property renders an increase in deformation or displacement of the free end and a reduction in frequency, noticed in the vicinity of the fixed end of the beams where maximum stresses are captured.

On the experimental side, PVDF film has shown to be a potential sensor which can be used for damage detection. The material has proven to be strong and durable during the fabrication and operating conditions. The damage detection procedure used can easily be implemented for structural analysis. It requires modest equipment, simple to operate which offers the advantage that measurements may be carried out in a real inspection case scenario where only few frequency modes are required to identify the damage. It is worth to mention that PVDF sensors are not appropriate for static or quasi-static experiments as the charge accumulated in the

film electrodes decays very rapidly with time. This aspect was confirmed during the tests, hence the reason why measurements with PVDF film are limited to dynamic conditions only. Under dynamic loading, the sensor was capable of differentiating the frequency from defect free to flawed beams with no need for signal amplification. The measurements taken were limited to the first natural frequency since it produces higher displacements with only one degree of freedom. The sensor's location along the composite beams was restricted to be near the fixed end to capture the high stresses produced by deformation. Good agreement was found between experimentally measured and numerically simulated results. However, there are still aspects of the sensor performance and its relation to monitoring the structure which need to be further investigated such as change in environmental conditions, sensor design and configuration. It was observed that the change in frequency from one flaw position to the other is not very high which might suggest that under the testing conditions set, the sensor is still not capable of entirely sensing the flaws in the beam. Therefore, an optimisation of the sensing capabilities in terms of signal processing would be a step ahead to consider prior to obtain more precise results.

6.3 Recommendations for Future Work

Based on the results of this study, it is suggested that future work could be focused on the following aspects:

- Investigation of different size and shape sensors (apart from rectangular) to determine their suitability of incorporation in to more complex structures
- Investigation of the sensor response in detecting damage in geometries more representative to real cases for example rectangular structures, membranes, three and four point loading beams etc.

The findings of this research can be considered as a starting point rather like a feasibility study for more in depth analysis of damage or defects in structures, using PVDF sensors.

REFERENCES

Bar – Cohen Y, Xue. T. & Lih. S, 1996. Polymer Piezoelectric Transducer for Ultrasonic NDE. *Jet Propulsion Laboratory, California Institute of Technology (NASA)*.NDTnet.1 (9)

Baskar M, Bhat M, and Murthy C, 2006. Structural Health Monitoring using Strain Gauges, PVDF and Fiber Bragg Grating Sensors: A Comparative Study. *Indian National Seminar on Non-Destructive Evaluation* (334-337).

Bois C, Hergoz P & Hochard C, 2006. Monitoring a Delamination Composite Beam using In-situ Measurements and parametric Identification. *Journal of sound and Vibration*. 299 (786-805)

Bray D, Stanley K, 1989. A Tool in Design, Manufacturing and Service. Non Destructive Testing and Evaluation. McGraw-Hill inc United States, p21-35

Chen. R.L & Wang. B, 2004. The use of PVDF films as sensors for experimental modal analysis of structures. *Journal of Smart Materials and Structures*.13 (791-799)

Cerri M, Vestroni F, 1999. Detention of Damage in Beams Subjected to Diffused Cracking. *Journal of Sound and Vibration*. 234 (2), 259-276

Frederic A.J 1997 *Damage Detection Based on the Geometric Interpretation of the Eigenvalue problem*. Thesis submitted in partial fulfillment of the requirements for the Doctor of Philosophy Degree Masters of Technology Degree in Engineering Science and Mechanics at the Virginia Polytechnic Institute and State University.

Gama A.L, Morikawa S.R, 2007. Monitoring Fatigue Crack Growth in Compact Tension Specimens Using Piezoelectric Sensors. *Journal of Experimental Mechanics* 48 (247-252)

George J, 2007. *Piezoelectric Sensing Capabilities of Polyinylidene Fluoride*: Application to a Fluid flow through a compliant tube. Aerospace Engineering, Texas A&M University

Ginsberg J.H, 2001. *Mechanical and Structural Vibrations*. John Wiley and Sons, Inc, p64-112

Harrison J.S, 2001. *Piezoelectric Polymers*. Icase Report 43, p1-7. NASA Langley

Research Center. Hampton, Virginia.

Huang J, 1998. *Overview of β- Polyvinylidene Fluoride and its use as a Piezoelectric Polymer*.[Online available]

Hertzberg R.W, 1996. *Deformation and Fracture Mechanics of Engineering Materials*. Fourth Edition, by John Wiley and Sons, p23-55

Ishak S, Liu G & Lim S, 2001. Locating and Sizing of Delamination using Computational and Experimental Methods. *Journal of Composites*, Part B, Vol 32, (287-298)

Keilers C, Chang F,1995. Identifying Delamination in Composites Beams using Built-in Piezoelectrics. *Journal of Intelligent Material Systems and Structures.* 5 (649–663).

Kaspar J.W, 2002. Constitutive Models for Engineering Materials. Encyclopedia of Physical Science and Technology. Third edition Vol 3, p603-633. University of Colorado at Boulder.

Kessler S, 2002. *Piezoelectric Based in-Situ Damage Detection of Composite Materials for Structural Health Monitoring Systems*. Dissertation submitted to the Department of Aeronautics and Astronautics in Partial Fulfillment of the Requirements for the Doctorate of Philosophy in Aeronautics and Astronautics at the Massachusetts Institute of Technology.

Kuang K.S, Quek S.T and Cantwell W.J, 2004. Use of Polymer-based Sensors for Monitoring the Static and Dynamic Response of a Cantilever Composite Beam. Journal of Materials science 39 (3839-3843)

Lin. B. & Giurgiutiu. V, 2006. Modeling and Testing of PZT and PVDF Piezoelectric Wafer Active Sensors. *Journal of Smart Materials and Structures*.15 (1085-1087).

Luo. H. & Hanagud. S. 1999 PVDF Film Sensor and its Applications in Damage Detection. *Jornal of Aerospace Engineering*.12 (23-26).

Lee C K and Moon F C 1990. Modal Sensors/Actuators *J*ournal of*. Applied Mechanics*. Vol 57 434–41

Malatkar P, 2003. *Non Linear Vibrations of Cantilever Beams and Plates*. Dissertation submitted to the Virginia Polytechnic Institute and State University for the Doctor of Philosophy degree in Engineering Mechanics, p20-35

Piezo Film Sensors. Technical Manual, 2006 *Measurement Specialties, Inc. Rev D*

Piezoelectric History, 2005. The Discovery by the Curie Brothers. Micromechatronics Inc. [Online Available]: *www.piezoelectrics.net/piezoelectrichistory.htm*

Preumont A, 1997. Vibration Control of Active Structures: *An introduction*, Kluwer academic publishers, Dordrecht, p32-49

Roseiro L, Ramos U, Leal R & Henriques J, 2003. Damage Detention of Laminated Composite Plates using Distributed Piezoelectric Sensors and Neural Networks. *Workshop on Smart Materials and Structures* p281-290

Saleh F, B Supriyadi, Suhendro B and Tran D, 2004. Damage Detection in Non-Prismatic Reinforced Concrete Beams Using Curvature Mode Shapes**.** *Structural Integrity and Fracture* [Online Available]: http://eprint.uq.edu.au/archive/00000836

Schaaf K, Rye P & Nemat-Nasser S, 2007. *Optimization of Sensor Introduction into Laminated Composites*. Proceedings of the 2007 SEM Annual Conference and Exposition on Experimental and Applied Mechanic University of California, San Diego, 9500 USA, p1-4

Scott W, Charles R, Michael B, 2003. *A Summary of Vibration-Based Damage Identification Methods*. Engineering Analysis Group, Los Alamos, p1-34

Shirinov A, Schomburg W, 2007. *Pressure Sensor from PVDF Film*. Aachen University, Konstruktion und Entwicklung von Mikrossystemen, Aachen Germany.

Srinivasan A.V, Mcfarland D.M. Smart Materials and Structures: *Analysis and Design*. Cambridge University Press 2001, p7-21

Stratton A, Pelegri A, 1999. *Investigation of Interlayer and Intralayer Delaminations* College of Engineering, Rutgers University. Piscataway, NJ

Sun B, 2003. Smart Materials and Smart Systems. *Lecture Notes*, p8-11. Cape Peninsula University of Technology. Centre for Research in Applied Technology, Cape Town

Sun. B, Qiu. Y, 2004. Analysis of Circular Shape Distributed Piezoelectric Actuators. *Journal of Composite Structures.* 62 (177-179).

Tan P,Tong L, 2003. A Delamination Detection Model for Composite Beams using PRFC Sensor/Actuator. *Journal of Composites* .Part A 35 (231-247).

Theodore J.R, 1998 . Overview of Composite Materials. Published by Chapman and Hall, London, p22-48

Vodicka R, Galea S, 1998. *Use of PVF sensors for health monitoring of bonded composite patches*. Published by DSTO Aeronautical and Maritime Research Laboratory, Melbourne Victoria, Australia, p1-14

Yang S, Hung C & Chen K 2005. Design and fabrication of a smart layer module in composite laminated structures. *Journal of Smart Materials and Structures*, 14 (2005) p315-320

Yee J, 2003.*Shock Resistance of Ferromagnetic Micromechanical Magnetometers*. A Thesis Submitted in Partial Satisfaction of the Requirements for the Degree of Master of Science in Electrical Engineering, p8-25

Yin L, M. Wang & Shen Y, 1994. Damage Monitoring in Composite Laminates by Piezoelectric Films. *Journal of Composites and Structures*, Vol 59 (623-630)

Willian J.G Constitutive Models for Engineering Materials: *Encyclopedia of Physical Science and Technology* 2002. University of Colorado at Boulder, Third Edition Vol 3, p42-48

Washington G, 2002. A New Materials Paradigm. The Ohio State University, p5-15. [Online available]

BIBLIOGRAPHY

Bailey T and Hubbard JE, 1985. Distributed Piezoelectric-Polymer for Active Control of a Cantilever Beam. *Journal of Guidance, control and dynamics*. 5 (605-611)

Ertug˘rul C, Orhan S & Murat L, 2004. An analysis of cracked beam structure using impact echo method. *NDT & International* 38 (368-373). Online available at: Science direct.com

Fellipa C.A. Variational Formulation of Plane Beam Element. *Lecture Notes*. University of Colorado at Boulder [Online available] http://www.colorado.edu/engineering/CAS/courses.d/IFEM.Ch13.pdf

Gadelrab R, 1996. The effect of delamination on the natural frequencies of a laminated composite beam. *Journal of Sound Vibrations*. 197 (283-292)

Huang D 1999. Approximate Analytical Solutions for Vibration Control of Smart Composite Beams. Thesis submitted in partial fulfillment of the requirements for Masters of Technology Degree in Mechanical engineering at the Cape Peninsula University of Technology. Cape Town, SA

Inman D.J 1996. *Engineering Vibration*. Prentice Hall, Englewood Cliffs, New Jersey, p329-370

Kattan P.I, Voyiadjis G.Z. Damage Mechanics with Finite Elements. Practical Applications with Computer Tools p37-45. [Online available]

Lee S, Park T, & Voyiadjis G, 2003. Vibration Analysis of Multi Delaminated Beams. *Journal of Composites*. Part B 34 (647-659)

Lennon B, Prendergast P, 2004.Modeling Damage Growth and Failure in Elastic Materials with Random Defect Distributions. *Mathematical Proceedings of the Royal Irish Academy*. 104A (2), 155-171.

Lestari W, Qiao P,2005. Damage detection of fiber-reinforced polymer honeycomb sandwich beams. *Journal of Composite Structures.* 67 (2005) 365–373

Mustapha F, Manson G, Worden K, & Pierce S, 2007. Damage location in an isotropic plate using a vector of novelty indices. *Journal of Mechanical Systems and Signal Processing.* 21 (2007) 1885–1906

Parnes R. Solid Mechanics in Engineering, 2001 by John Wiley and Sons, LTD, p496-525

Qiao. P, Lu. K. & Lestari. W, 2006. Curvature Mode Shape-Based Damage Detection in Composite Laminated Plates. *Journal of Composite Structures* 80 (409-428).

Roylance D. Mechanics of Materials, 1996 by John Wiley and Sons, Inc, p108-120

Shane C, 2006. Structural Health Monitoring Using Linear and Non-Linear Time Domain Methods. Department of Mechanical and Aeronautical Engineering, Clarkson University p1-10

Sunar M, Al-Bedoor B, 2007. Vibration Measurement of Cantilever Beam using Segmented Piezoelectric Sensor. *Journal of Mechanical Engineering Science*. Vol 222 (147-160)

Sun K.E., 2006. Design *and Characterization of Passive Wireless Strain Sensor*. A Thesis submitted in partial fulfillment of the requirements of the Masters of Science degree in Mechanical Engineering at the University of Puerto Rico. [Online available]: http://grad.uprm.edu/tesis/Kesun.pdf [12/07/2007].

University of Alberta. Dynamic Analysis using Ansys. [Online available] http://www.mece.ualberta.ca/tutorials/ansys/.html

APPENDIX A: EXPERIMENTAL MEASUREMENTS FOR FREE END DISPLACEMENT UNDER STATIC LOADING

Flaw position: X_i = 0 (Beam A)				
Load (N)	**w_1 (mm)**	**w_2 (mm)**	**w_3 (mm)**	**AVERAGE**
0	0	0	0	**0**
0.4905	0.64	0.63	0.64	**0.64**
0.981	1.27	1.27	1.26	**1.27**
1.4715	1.92	1.92	1.92	**1.92**
1.962	2.55	2.54	2.55	**2.55**
2.4525	3.19	3.18	3.19	**3.19**
2.943	3.83	3.82	3.83	**3.83**

Flaw position: X_i = 47.5mm (Beam B)				
Load (N)	**w_1(mm)**	**w_2 (mm)**	**w_3 (mm)**	**AVERAGE**
0	0	0	0	**0**
0.4905	0.66	0.65	0.66	**0.66**
0.981	1.33	1.33	1.33	**1.33**
1.4715	1.99	2.01	1.98	**1.99**
1.962	2.66	2.65	2.67	**2.66**
2.4525	3.32	3.32	3.31	**3.32**
2.943	3.99	3.98	4	**3.99**

Flaw position: X_i = 82.5mm (Beam C)				
Load (N)	**w_1 (mm)**	**w_2 (mm)**	**w_3 (mm)**	**AVERAGE**
0	0	0	0	**0**
0.4905	0.66	0.67	0.65	**0.66**
0.981	1.31	1.32	1.31	**1.31**
1.4715	1.96	1.96	1.96	**1.96**
1.962	2.62	2.61	2.63	**2.62**
2.4525	3.27	3.27	3.26	**3.27**
2.943	3.93	3.92	3.93	**3.93**

Flaw position: X_i = 117.5mm (Beam D)				
Load (N)	**w_1 (mm)**	**w_2 (mm)**	**w_3 (mm)**	**AVERAGE**
0	0	0	0	**0**
0.4905	0.65	0.66	0.64	**0.65**
0.981	1.28	1.28	1.29	**1.28**
1.4715	1.94	1.95	1.93	**1.94**
1.962	2.58	2.58	2.58	**2.58**
2.4525	3.23	3.22	3.23	**3.23**
2.943	3.86	3.86	3.85	**3.86**

Static Displacement Measurements and Calculated Apparent Elastic Modulus								
Load (N)	**Beam A (mm)**	**E(GPa)**	**Beam B (mm)**	**E(GPa)**	**Beam C (mm)**	**E(GPa)**	**Beam D (mm)**	**E(GPa)**
0	0	0	0	0	0	0	0	0
0.491	0.64	1.75E+09	0.66	1.68E+09	0.66	1.71E+09	0.65	1.73E+09
0.981	1.27	1.75E+09	1.33	1.68E+09	1.31	1.70E+09	1.28	1.73E+09
1.472	1.92	1.75E+09	1.99	1.68E+09	1.96	1.71E+09	1.94	1.73E+09
1.962	2.55	1.75E+09	2.66	1.68E+09	2.62	1.71E+09	2.58	1.73E+09
2.453	3.19	1.75E+09	3.32	1.68E+09	3.27	1.70E+09	3.23	1.73E+09
2.943	3.83	1.75E+09	3.99	1.68E+09	3.93	1.70E+09	3.86	1.73E+09
	AVERAGE	**1.75E+09**		**1.68E+09**		**1.71E+09**		**1.73E+09**

APPENDIX B: EXPERIMENTAL MEASUREMENTS UNDER DYNAMIC LOADING

MEASUREMENTS FOR FIRST NATURAL FREQUENCY IN TIME AND FREQUENCY DOMAIN (Hz)				
Test No.	**Beam A**	**Beam B**	**Beam C**	**Beam D**
1 - TD	56.66	55.23	55.84	56.22
2 - TD	56.66	55.23	55.84	56.22
3 - TD	56.66	55.23	55.84	56.22
4 - TD	56.66	55.23	55.84	56.22
5 - TD	56.66	55.23	55.84	56.22
6 - TD	56.66	55.23	55.84	56.22
7 - TD	56.66	55.23	55.84	56.22
8 - TD	56.66	55.23	55.84	56.22
9 - TD	56.66	55.23	55.84	56.22
10 - TD	56.66	55.23	55.84	56.22
11 - FD	56.69	55.27	55.88	56.28
12 - FD	56.69	55.27	55.88	56.28
13 - FD	56.69	55.27	55.88	56.28
14 - FD	56.69	55.27	55.88	56.28
15 - FD	56.69	55.27	55.88	56.28
16 - FD	56.69	55.27	55.88	56.28
17 - FD	56.69	55.27	55.88	56.28
18 - FD	56.69	55.27	55.88	56.28
19 - FD	56.69	55.27	55.88	56.28
20 - FD	56.69	55.27	55.88	56.28
AVERAGE	**56.68**	**55.25**	**55.86**	**56.25**

APPENDIX C: FE RESULTS FOR BEAMS UNDER STATIC LOADING

Flaw Position: X_i = 0		Flaw position: X_i = 23.75mm		Flaw position: X_i = 47.5mm	
Load (N)	**a_2-a_1=0**	**Load (N)**	**a_2-a_1=35mm**	**Load (N)**	**a_2-a_1=35mm**
0	0	0	0	0	0
0.4905	0.625	0.4905	0.652	0.4905	0.644
0.981	1.250	0.981	1.304	0.981	1.288
1.4715	1.875	1.4715	1.956	1.4715	1.932
1.962	2.500	1.962	2.608	1.962	2.576
2.4525	3.126	2.4525	3.260	2.4525	3.220
2.943	3.751	2.943	3.912	2.943	3.864

Flaw position: X_i = 82.5mm		Flaw position: X_i = 117.5mm	
Load (N)	**a_2-a_1=35mm**	**Load (N)**	**a_2-a_1=35mm**
0	0	0	0
0.4905	0.635	0.4905	0.629
0.981	1.270	0.981	1.259
1.4715	1.905	1.4715	1.889
1.962	2.540	1.962	2.519
2.4525	3.175	2.4525	3.149
2.943	3.810	3.821	3.779

APPENDIX D: FE RESULTS FOR BEAMS UNDER DYNAMIC LOADING

X_i (mm)	$a_2 - a_1$ (m)	Natural frequency (Hz)
0	0	53.3
0.02375	0.035	50.63
0.0475	0.035	51.75
0.0825	0.035	52.76
0.1175	0.035	53.09